RUPRECHT-KARLS-
UNIVERSITÄT
HEIDELBERG

HHN
HOCHSCHULE HEILBRONN
TECHNIK WIRTSCHAFT INFORMATIK

Studiengang Medizinische Informatik

BACHELOR THESIS

# Brain Computer Interfaces

## *OpenViBE as a Platform for a P300 Speller*

Herbert S. Kisakye

Matrikelnummer: 172588

E-Mail: hkisakye@stud.hs-heilbronn.de

Heilbronn August 6, 2012

Supervisors: Prof. Dr. Rolf Bendl

Dipl.-Inform. Med. C. Maier

## ACKNOWLEDGEMENTS

This thesis is based on research I did in the Bio-Signal Laboratory at the Heilbronn University of Applied Sciences, in the summer of 2012. Without the help of different individuals I would never have been able to achieve much

I am greatly indebted to *Dipl.-Inform. Christoph Maier* , for his readiness to take time out of his busy schedule, working on his Doctorate, to answer questions and give me invaluable guidance.

I would like to thank *Prof.Dr. Rolf Bendl* immensely, for pointing me in this direction of a relatively new yet exciting field.

Of course this work would never have come to fruition without the people, mostly fellow students at the university, that sat through many hours of repetitive, sometimes monotonous experiments and those that helped with a few technical aspects. Thank you all so much.

Lastly a special thank you to all my friends and family for the emotional support. You kept me going.

Herbert Sunday Kisakye

## Abstract

Aside from hardware, a major component of a Brain Computer Interface is the software that provides the tools for translating raw acquired brain signals into commands to control an application or a device. There's a range of software, some proprietary, like MATLAB and some free and open source (FOSS), accessible under the GNU General Public License (GNU GPL). OpenViBE is one such freely accessible software. This thesis carries out a functionality and usability test of the platform, looking at its portability, architecture and communication protocols. To investigate the feasibility of reproducing the P300 xDAWN speller BCI presented by OpenViBE, users focused on a character on a 6x6 alphanumeric grid which contained a sequence of random flashes of the rows and columns. Visual stimulus is presented to a user every time the character they are focusing on is highlighted in a row or column. A TMSi analog-to-digital converter was used together with a 32-channel active electrode cap (actiCAP) to record user's Electroencephalogram (EEG) which was then used in an offline session to train the spatial filter algorithm, and the classifier to identify the P300 evoked potentials, elicited as a user's reaction to an external stimulus. In an online session, the users tried to spell with the application using the power of their brain signal. Aspects of evoked potentials (EP), both auditory (AEP) and visual (VEP) are further investigated as a validation of results of the P300 speller.

## List of Abbreviations

| | |
|---|---|
| ADC | Analog Digital Converter |
| EEG | Electroencephalogram |
| ECG/EKG | Electrocardiogram |
| EMG | Electromyogram |
| ECoG | Electrocardiogram |
| CNS | Central Nervous System |
| DFT | Discrete Fourier Transformation |
| FFT | Fast Fourier Transformation |
| LDA | Linear Discriminant Analysis |
| EP | Evoked Potentials |
| V/A-EP | Visual/Auditory- Evoked Potentials |
| SSVEP | Steady State Visual Evoked Potentials |
| BCI | Brain-Computer Interfaces |
| SNR | Signal to Noise Ratio |
| GUI | Graphical User Interface |
| VR | Virtual Reality |
| fMRI | Functional Magnetic Resonance Imaging |
| NIRS | Near-Infrared Spectroscopy |

# Table of Contents

# 1 Introduction: Human Computer Interaction

## 1.1 Overview

We live by interacting with the physical world around us. This interaction normally involves thought and action. The brain, through its output pathways; the peripheral nervous system and muscles, controls motor movement. This way we are able to move our arms, legs or any part of the body as a means of communication or performing day-to-day tasks – if we are healthy.

However, people with severe neuromuscular injuries such as after an accident or those suffering from neurodegenerative diseases like Amyotrophic Lateral Sclerosis (ALS), brainstem stroke or cerebral palsy soon lose part or all of this voluntary muscular activity, the communication path between brain and effector muscles having been cut off, leaving only the cognitive function intact. This in medical terms is referred to as the locked-in syndrome: sufferers are left fully conscious of their surroundings but with little to no mobility in their bodies, making it impossible for them to live without external help.

Advances in the fields of neuroscience, brain imaging technologies and computing have provided us with the opportunity to directly interface the brain with a computer [1] thereby creating a communication and control system that bypasses peripheral nerves and muscles to enable interaction through brain activity alone: the brain-computer interface (BCI).

BCIs can enable locked-in patients to still interact with their environment by solely harnessing the power of their brain activity. Devices including spelling applications for communication, input and navigation on a computer system such as moving a cursor or controlling a robotic arm have been tested with success.

Real-time brainwave activity is beginning to be used to control digital movies, turn on music and switch lights on and off and to control virtual objects like an avatar[1] [2], [3], [4], [5] Messages are conveyed by spontaneous or evoked EEG activity rather than by muscles contractions. In years to come, scientists want to reconnect the brain to paralyzed limbs to enable them to function again.

[1] http://en.wikipedia.org/wiki/Avatar_(computing)

By integrating such applications into the routines of such patients as a method of assisted living, their quality of life can be greatly improved through giving them more independence as well as emotional stability.

## 1.2 Aim and scope of the thesis

The Heilbronn University of Applied Sciences (Hochschule Heilbronn) has recently acquired equipment that can be used for recording the Electroencephalogram (EEG) in the Bio-Signals Laboratory. These devices come with a fairly high price tag. The idea was to take advantage of the availability of non-proprietary open source software for real-time processing of brain signals, integrate it with the acquisition device and build a functional laboratory-based BCI application: the P300 visual speller.

Currently there are not fewer than 10 such open source BCI platforms. Among them, OpenViBE was chosen basing on the functionality and usability analysis (See chapter 2) and the OpenViBE website [6].

## 1.3 The BCI Framework

### 1.3.1 Principle of the BCI

A typical BCI system involves acquisition of electrical signals from the brain's neuron activity and transforming them into commands to control an application. The user's brain activity is recorded using a single or multiple electrodes attached to the scalp for the EEG or directly onto the cortex, by surgical means, for the ECoG. Another method is to use depth electrodes implanted in the brain. The most common BCIs are EEG-based, as they are not only cheaper but also easier to set up.

The acquired EEG signal is digitized by an analog-to-digital converter and fed into a computer for processing. Different characteristics can be observed in this ongoing oscillatory activity depending on varying degrees of the user's mental or physical state (a relaxation EEG is different from the one recorded when the subject is performing a mental activity for example). Specific features like amplitudes of evoked

potentials are extracted and passed to translation algorithms for training. After a training period, the algorithms are able to identify these specific features (data mining and machine learning) in a subsequent ongoing EEG, which they can classify and translate into commands (which reflect the user's intent) to control a simple word processing program, a robotic arm, control a wheel chair or any such devices (Figure 1.1). This process involves little to no muscular activity and can be understood as an interface between the brain and an application.

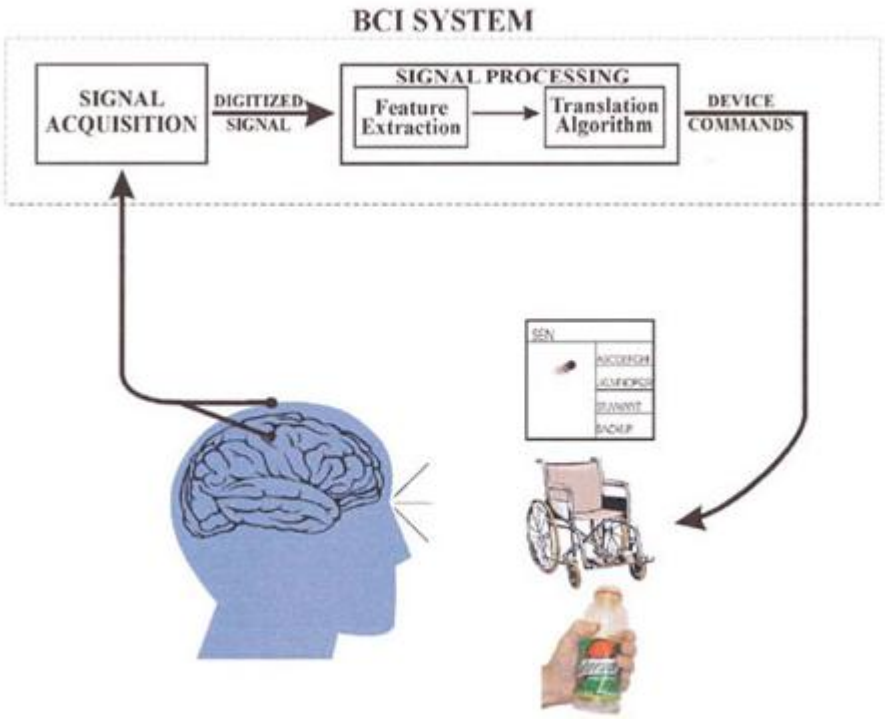


**Figure 1.1: Illustration of a simple Brain-Computer Interface [7]**

BCIs can use signal features in the time domain, like amplitudes of evoked potentials or those in the frequency domain like mu (μ) and beta range (β) amplitudes [7] employed in motor imagery[2] BCIs.

### 1.3.2 Integrating Biofeedback

Bruce Eugene [8] defines feedback as sensing of the output of a system and transmission of this signal back to the system input in order to influence the future output of the system. Through biofeedback, the user learns to control those features of the signal that reflect his or her intent by selectively influencing the amplitude and

[2] Imagined movement causes the same brain activity as real movement: signals to control hand/leg BCIs like prosthetics and game control can be realized through thought.

power of their output. According to Birbaumer [9], most of the clinical BCI studies in human patients use feedback of EEG oscillations or of event-related potentials (ERPs). The subject receives visual or auditory online feedback of his or her brain activity and tries to voluntarily modify a particular type of brain wave: this is known as self-regulation (Figure 1.2).

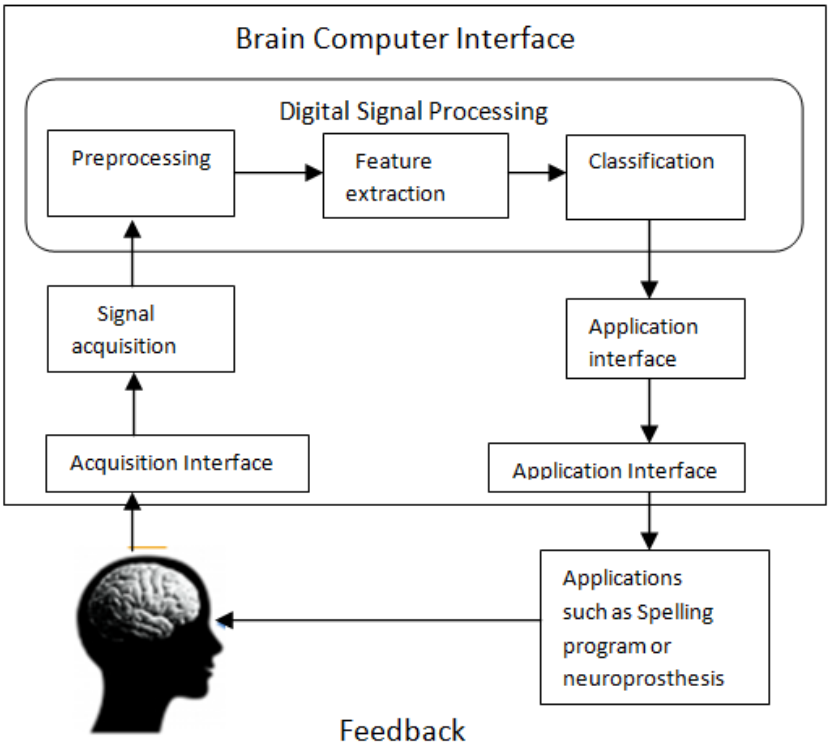


**Figure 1.2: A block diagram of a Brain-Computer Interface. Adopted from [5]**

Sörnmo et al [5] found that the EEG exhibits variability due to factors such as time of the day, fatigue and hormonal level. The training phase of the user and that of the algorithms may not be a onetime event but may need to be repeated on a regular basis in order to achieve good performance. The user must develop and maintain good correlation between their intent and the features the algorithms extract for use in the BCI application.

### 1.3.3 History of the BCI

BCI is a relatively new field. Research started several decades after Hans Berger first discovered the electroencephalogram in the 1920s. In the 1960s, applying easy-to-use noninvasive methods, studies were done on the development of neuro-feedback in which monkeys would learn to voluntarily increase or decrease the power of their alpha waves, the predominant amplitudes in an EEG. They (monkeys) learnt to increase or decrease firing rates of the neurons in the motor cortex and could move a prosthetic arm simply by thinking about it.

In the 1970s, **Jacques Vidal** published his work on a government sponsored research in bio cybernetics and human computer interactions, at the University of California Los Angeles (UCLA) Brain Research Institute. He showed how brain signals could be used to build up a mental prosthesis [10]. He is also credited with coining the term Brain-Computer Interfaces[3].

Lawrence Farwell and Emanuel Donchin developed an EEG-based BCI. In Talking off the top of your Head, published in 1988 [11], they outline an algorithm used in the decision making process of a P300 speller to identify target and non-target potentials in an ongoing EEG signal. This was the first time event related potentials (ERPs) were used in a BCI application.

### 1.3.4 Other Methods of Signal Acquisition

Signal acquisition for BCIs can be grouped into two, depending on whether a surgical procedure is required to implant electrodes in/on the brain to measure its electrical activity or not. Non-invasive methods require no surgery. However not all acquisition procedures involve the use of electrodes; some, like fMRI measure electrical activity by use of blood oxygenation level dependence (BOLD). The table below summarizes the different methods

[3] . http://www.cs.ucla.edu/~vidal/vidal.html

**Table 1: Signal acquisition methods in BCIs**

| Method | Measured quantity | Invasive |
|---|---|---|
| EEG | Electrical potential | No |
| ECoG | Electrical potential | Yes |
| Micro-electrodes | Electrical potential | Yes |
| MEG | Magnetic field | No |
| fMRI | BOLD | No |
| NIRS | BOLD | No |

**Adapted from D'Albis** [12]

### 1.3.5 Classification of BCIs

There's no standard classification for BCIs. In some literature the acquisition modes are used, thus invasive and non-invasive BCIs. Other classifications are:

I. Synchronous/Asynchronous BCIs
II. Cued/Spontaneous BCIs
III. Dependent/Independent BCIs

*Dependent vs Independent:* Although it uses brain signals, a dependent BCI will still require the user to apply part of his/her peripheral system. A BCI built on visual stimuli involves the movement of the user's eyes (and muscles). On the other hand independent BCIs rely on signals that can be triggered without involvement of muscle activity: with audio stimuli the tasks only involve thinking.

*Endogenous vs Exogenous:* In endogenous BCI, a user spontaneously generates the brain signal used for control while in exogenous BCI the signal is generated as a

response to an external stimulus such as AEPs and VEPs. Exogenous systems do not require extensive training of the user compared to endogenous ones and are easier to set up. Endogenous BCIs often require the use of neural-feedback to enable the user to learn to generate specific wave patterns like slow cortical potentials or sensorimotor rhythms. Their advantage is that severely affected persons can learn to operate them [13].

*Synchronous vs Asynchronous:* Asynchronous BCIs analyze an EEG patterns in a predefined time window leaving out anything that comes before or after. The user is only supposed to send commands during epochs determined by the system. Synchronous BCIs employ detection of specific events through continuous analysis of the user's EEG. It offers a more natural interaction for the user.

## 1.4 Physiology of the EEG

### 1.4.1 Background

Recorded work on neurophysiology goes back nearly 200 years to Carlo Matteucci (1811- 1868) and Emil Du Bois-Reymond (1818-1896) who were the first to register electrical signals emitted from muscle nerves using a galvanometer. The discoverer of the existence of human EEG signals however was Hans Berger (1873-1941), a German neurologist and psychiatrist. In 1929 he presented a report that included the alpha rhythm (8 – 13 HZ) as the major component of the EEG signals [14]. Work by other scientists in Europe and America, in the quest to understand the functioning of the brain and the central nervous system, the causes of diseases like brain tumors or epilepsy and finding treatment for them, has led to modern day methods of recognition, diagnosis and treatment, used in clinical encephalography [15]. This correlates CNS functions as well as dysfunctions and diseases with certain patterns of the EEG.

### 1.4.2 Electrical Activity in the Brain

Brain tissue is made up of three components: 1. **neurons** (nerve cells), 2.**glial cells**, located between neurons, and 3.**extracellular space**, which is made up of mainly fluid containing other macro molecules. Glial cells make up the myelin sheath, which protects the axon. Neurons are responsible for intracellular and intercellular signaling which they do by generating and transmitting electrochemical impulses as a response to stimuli. The human brain contains over 25 billion neurons. Typically the neuron consists of dendrites, which act as receptors for signals from other neurons, a cell body and the ending called an axon. The axon is attached to other nerve cells through their dendrites or axon to form a synapse. The synapse acts as an interface between nerve cells. In the human brain, each nerve cell is connected to approximately 10.000 other nerve cells, mostly through dendritic connections. [16], [14], [17]

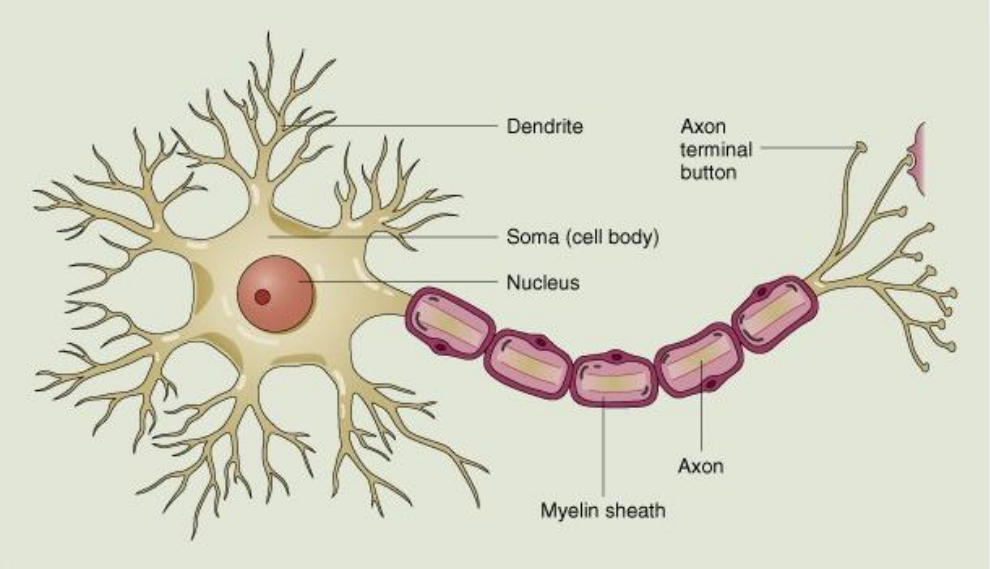


**Figure 1.3: Structure of a neuron**[4]

The dendrites, together with the cell body and part of the initial piece of the axon are the input surfaces of the cell (Figure 1.3). Impulses received through the dendrites are transported along the axon to its terminal branches through to the synapse where they are picked up by other connected neurons.

[4] Source:http://springvisualculture1b.blogspot.de/

### 1.4.3 Neuron Activity

The central nervous system (CNS) is generally an interconnection of neurons and glial cells to create a communication network of both chemical and electrical activity. The activities in the CNS are mainly related to the synaptic currents transferred between the junctions (synapses) of axons and dendrites, or dendrites and dendrites of cells. A negative potential of (60-70 mV) may be recorded under the membrane of the cell body compared to the extracellular environment. This potential changes with variations in synaptic activities relating to distributions of $Na^+$, $K^+$ and $Cl^-$ across the membrane (Figure 1.5). If an action potential travels along the fiber, which ends in an *excitatory* synapse, an excitatory post-synaptic potential (EPSP) occurs in the following neuron. If two action potentials travel along the same fiber over a short distance, there will be a summation of EPSPs producing an action potential on the post-synaptic neuron providing a certain threshold of membrane potential is reached. If the fiber end in an *inhibitory* synapse then hyper polarization will occur, indicating an inhibitory postsynaptic potential (IPSP)

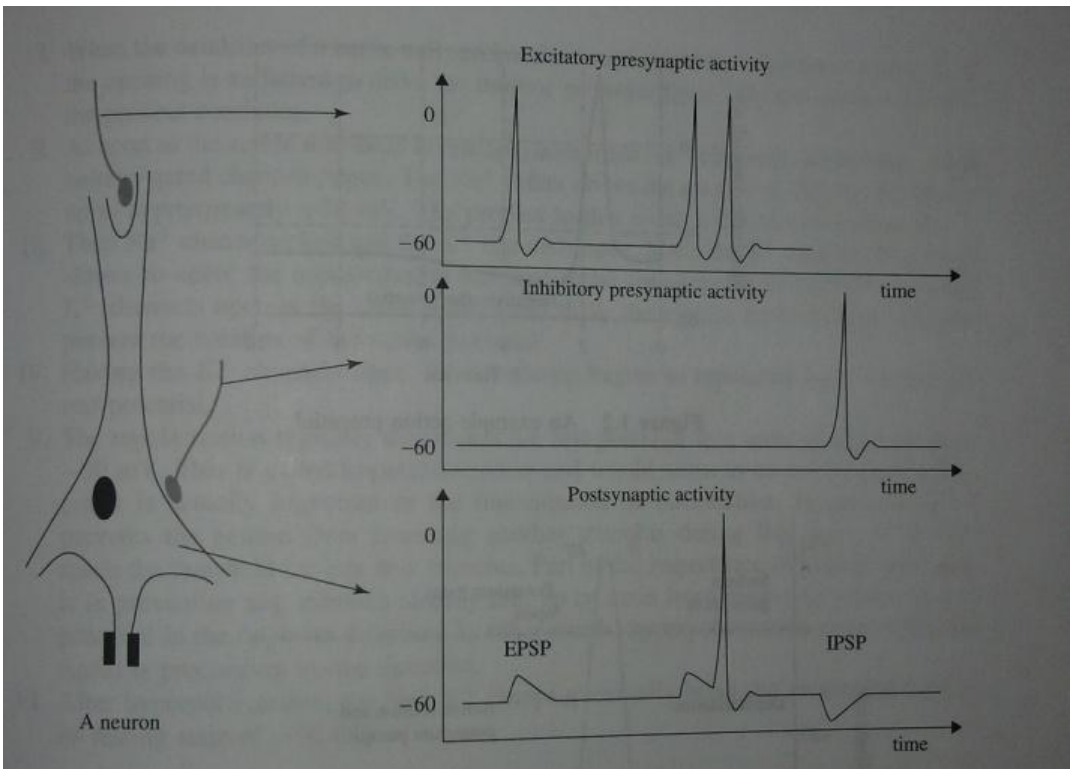


**Figure 1.4: The neuron membrane potential changes and current flow during synaptic activation recorded by means of intracellular microelectrodes ( [14])**

Following the generation of IPSP (hyper polarization), there is an overflow of cations (+ve particles) from the nerve cell into the extracellular space or an inflow of anions (-ve particles) into the nerve cell (figure 1.4). This flow ultimately causes a change in potential along the cell membrane. Primary currents generate secondary currents along the cell membrane in the intra- and extracellular space. The portion of these currents that flow through the extracellular space is directly responsible for the generation of field potentials. These field potentials, usually with frequencies of up to 100 Hz are called EEGs if they possess a constant signal average. If there are slow drifts in the average signals this results into DC potentials which may mask the EEG [16], [14], [5].

### 1.4.4 Action Potentials

Transmission of information from one neuron to another takes place at the synapse; the signal, initiated in the soma, propagates through the axon as a short pulse called the action potential (AP). Although the initial signal is electrical, it is converted in the presynaptic neuron to a chemical signal (neurotransmitter) which diffuses across the synaptic gap and is subsequently reconverted to an electrical signal in the postsynaptic neuron. APs are initiated by many different types of stimuli; sensory nerves respond to many types of stimuli, such as chemical, light, electricity, pressure, touch, and stretching. Conversely, nerves in the CNS are mostly stimulated by chemical activity in the synapses.

A stimulus must be above a threshold level to cause the neuron to fire an AP. Very weak stimuli cause a small local electrical disturbance, but do not produce a transmitted AP. This results in the neuron acting as an ON/OFF-switch. As soon as the stimulus strength goes above the threshold, an action potential appears and travels down the nerve.

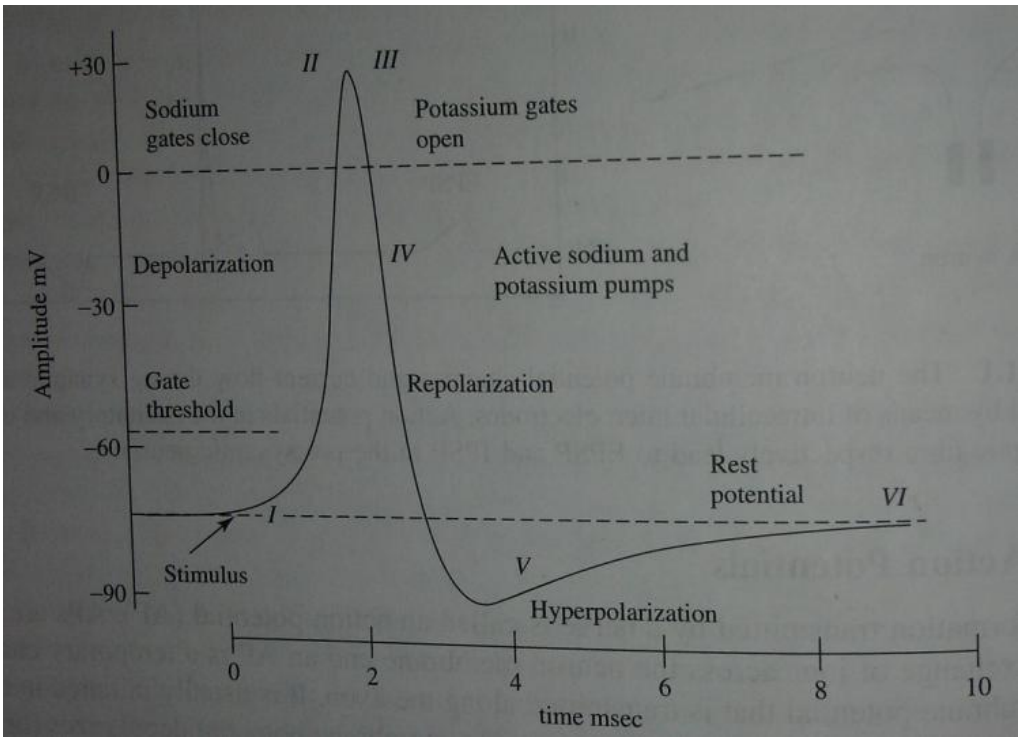


**Figure 1.5: Changing the membrane potential of a giant squid by closing the $Na^+$ channels and opening $K^+$ channels ( [14])**

Not all neurons contribute to the excitation of the postsynaptic neuron; inhibitory effects can also take place due to a particular chemical structure associated with certain neurons. A postsynaptic neuron thus receives signals which are both excitatory and inhibitory, and its output depends on how the input signals are summed together [14] [5].

The intensity of the input signals is modulated by the firing rates of the action potentials. High firing rate in the sensory neurons is associated with considerable pain or, in motor neurons, with powerful muscle contraction [5]

### 1.4.5 Characteristic Frequency Bands of the EEG

The EEG has a typical amplitude of about 2 – 100 µV and a frequency spectrum of 0.1 – 60 Hz. In healthy adults, the amplitudes and frequencies found in the EEG change from one state of a human to another, such as wakefulness and sleep. There

are five major brain waves (Figure 1.6) distinguished by their different frequency ranges and the power they contain.

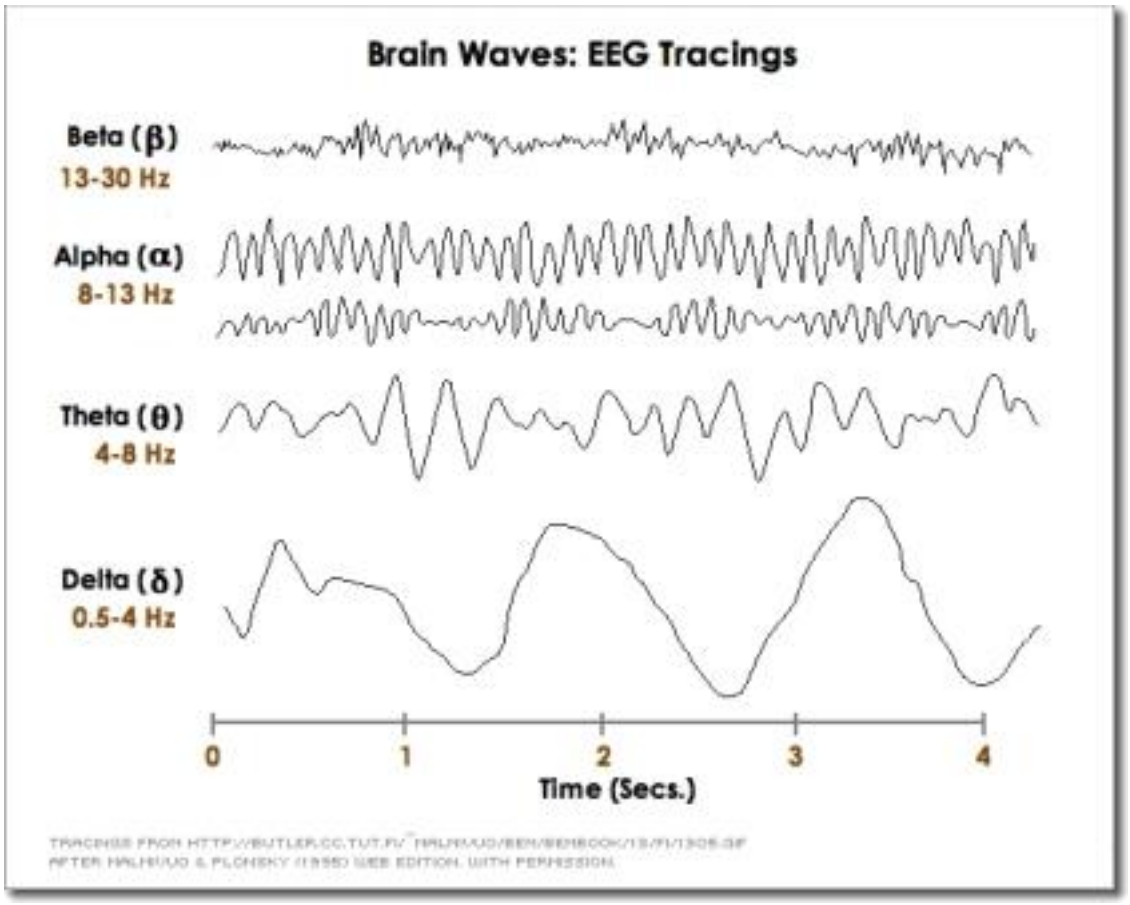


Figure 1.6: Typical encephalographic rhythms and their frequencies [18]

**Alpha (α) rhythm, 8 – 13 Hz:** This rhythm is most prominent in normal subjects who are relaxed and awake; the activity is suppressed when the eyes are open. The largest amplitude of this rhythm can be measured in the occipital region of the brain.

**Beta (β) rhythm, 14 – 30 Hz:** This is a fast rhythm with low amplitude, associated with an activated cortex and which can be observed, for example, during certain sleep stages. The beta rhythm is typically observed in the frontal and central regions of the scalp.

**Delta (δ) rhythm, < 4 Hz:** This rhythm is typically encountered during deep sleep and has large amplitude, thus low frequency. It is usually not observed in the wake, normal adult, but is indicative of cerebral damage or brain disease (encephalopathy)

**Gamma (γ) rhythm, > 30 Hz:** The gamma rhythm is related to a state of active information processing of the cortex. Using an electrode located over the sensorimotor area, this rhythm can be observed during finger movements.

**Theta (θ) rhythm, 4 – 7 Hz:** This rhythm mainly occurs during drowsiness and in certain stages of sleep.

High-frequency/low-amplitude rhythms reflect an active brain associated with alertness or dream sleep, while low-frequency/large-amplitude rhythms are associated with drowsiness and non-dreaming sleep states [5] [14]

### 1.4.6 Geography of the EEG Waves: Mapping Function to Region

Most of the neural activity is distributed near or around the outer surface of the brain, the cerebral cortex. It is perhaps the most important part of the CNS and the different regions of the cortex are responsible for processing vital functions such as sensation, learning, voluntary movement, speech and perception (figure 1.7).

Voluntary movement is primarily controlled by the area of the frontal lobe, just anterior to the central sulcus-the motor cortex. The motor cortex controls tasks requiring considerable muscle control, e.g. speech, facial expressions and finger movements. Sensory information is processed in various parts of the lobes; auditory in the superior parts of the temporal lobe, the visual cortex being situated at the posterior part of the occipital lobes, and the somatic sensory being located just posterior to the central sulcus of the parietal lobe.

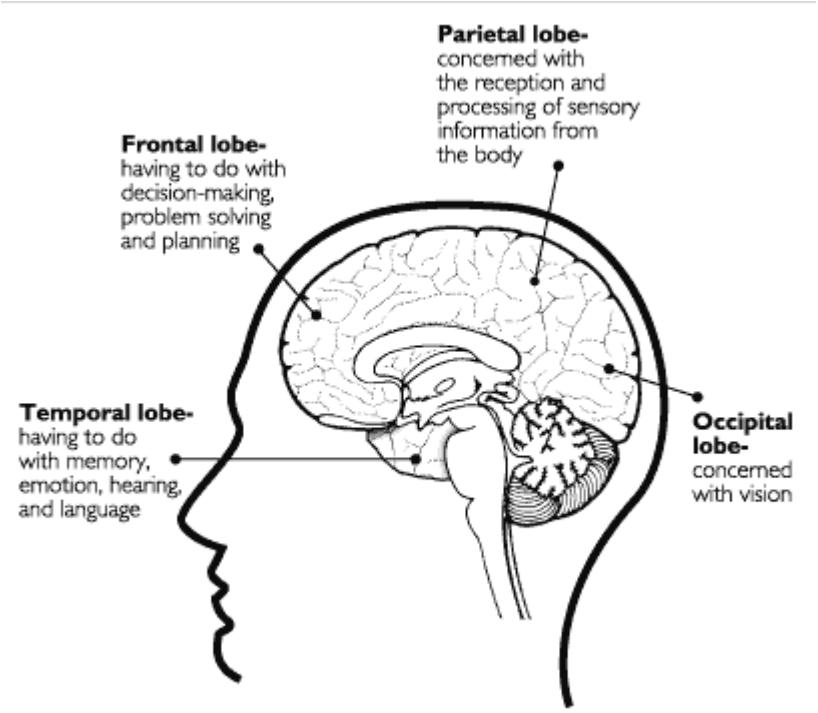


**Figure 1.7: A functional map of the cerebral cortex**[5]

## 1.5 Generation and Measurement of EEG

### 1.5.1 Generation in the brain

Collective activity of millions of cortical neurons produces an electrical field, which is sufficiently strong to be measured on the scalp. The electrical field is mainly generated by currents that flow during synaptic excitation of the dendrites, the excitatory postsynaptic potentials. In the cerebral cortex this current flow generates a magnetic field measurable by Electromyogram (EMG) and a secondary electrical field over the scalp measurable by EEG systems. The amplitude of the EEG signal is related to the degree of synchrony with which the cortical neurons interact: synchronous excitation produces a large amplitude signal on the scalp because the signals from individual neurons will add up in a time-coherent fashion, while asynchronous produces irregular looking EEG with low amplitude waveforms [14], [5].

[5] Source:http://www.wpclipart.com/

### 1.5.2 Electrode positioning

Clinical EEG is measured using the 10-20 International standardized system for electrode placement. The montage is with electrodes attached to the scalp at locations defined by certain anatomical reference points; the numbers 10 and 20 signify relative distances between different electrode locations on the skull surface [5]. Electrode placements (Figure 1.8) are labeled according to adjacent brain areas: F(frontal), C(central), T(temporal), P(posterior), O(occipital) [19]. The numbering represents left lobe (odd) and right lobe (even)

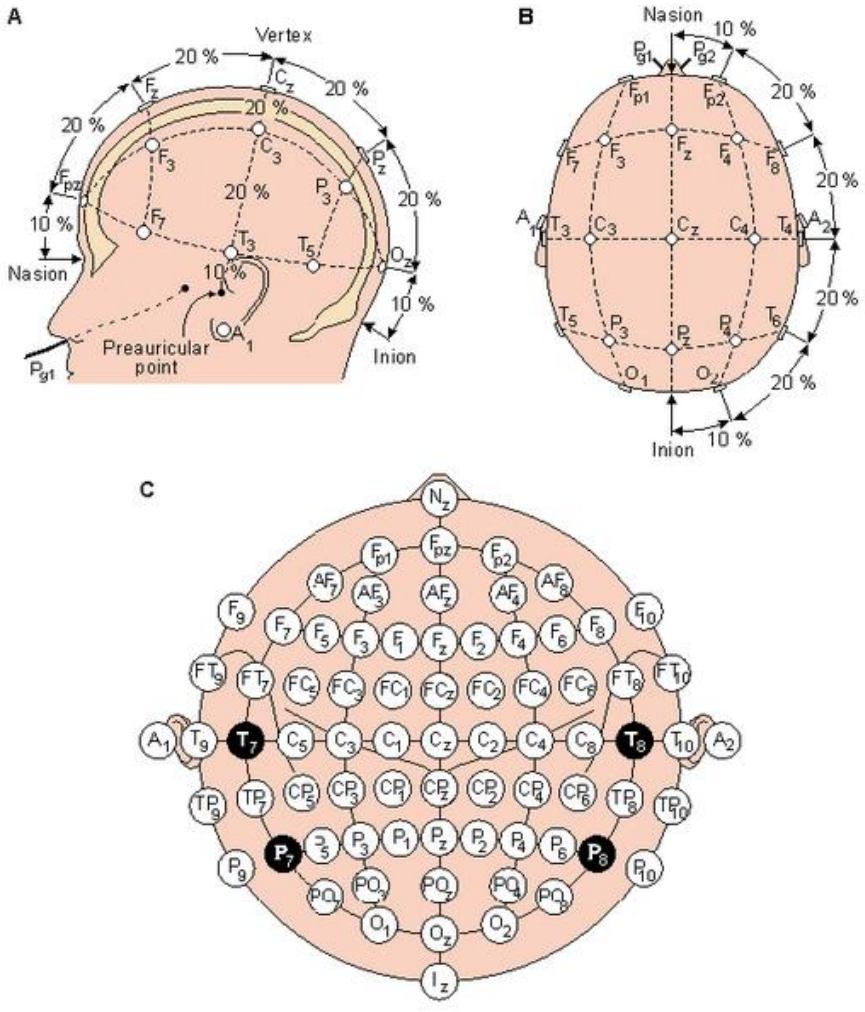


**Figure 1.8: Original 10-20 elecrode placement system with 19 electrodes (B) the extended one has 70 (C). Adopted from ( [20])**

The actiCAP used in the experiments here follows the 10-20 system (see 3.1-Hardware) however it follows an extended 32-active-electrode configuration with added Reference and Ground.

### 1.5.3 Montage and measurement modes

For all EEG acquisition in the experiments, a variation of the montage shown in figure 1.9 was used: used electrodes are marked in yellow (see 4.1.2, 4.2.1 and 4.2.2).

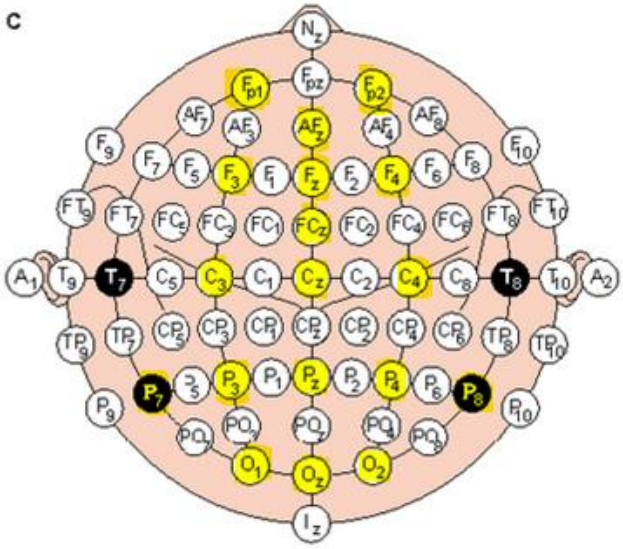


**Figure 1.9: Positions of electrodes used for acquisition in the experiments [20]**

Besides the international 10-20 system, many other electrode placement systems exist for recording electric potentials on the scalp. Measurement of evoked potentials is usually done using either *unipolar* or *bipolar* placement. Bipolar measures the potential difference between two electrodes while unipolar measures the potential of an electrode referenced to a neutral electrode or to the average of all electrodes [21]. These two techniques are depicted in figure 1.10 below.

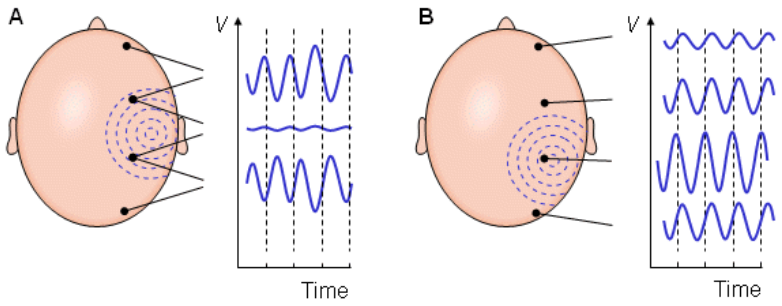


**Figure 1.10: Illustration of (A) Bipolar and (B) Unipolar modes of measurement**[6]

[6] Source: http://www.bem.fi/book/index.htm

# 2 The OpenViBE Platform

## 2.1 Overview

OpenViBE is a free and open source software platform for designing, testing and using Brain Computer Interfaces. The platform consists of a set of software modules that can be easily and efficiently integrated to develop fully functional BCIs for both real and virtual reality applications [22] [23].

Developed at the French National Institute for Research in Computer Science and Control (INRIA), OpenViBE is licensed under the GNU Lesser General Public License (version 2 or later) The platform is updated every 3 months (current version 0.14.03)

**Modularity and Reusability:** The platform is a set of software modules devoted to the main aspects of signal processing in BCI applications. These include: acquisition, pre-processing, processing and visualization of cerebral data, as well as enabling interaction with VR displays. Thanks to the box concept, users can easily add new software modules to suit their needs.

**Different Types of Users:** Tools were designed for different types of users; VR developers, clinicians, BCI researchers, neurologists etc. can use the platform, depending on their programming skills and knowledge in brain processes.

**Portability:** OpenViBE operates independently of software targets and hardware devices. An abstract level of representation allows it to be run with acquisition hardware such as EEG or MEG

**Connection with Virtual Reality:** The software can be integrated with high-end VR applications throught the Virtual Reality Peripheral Network (VRPN) server. OpenViBE acts as an external peripheral (client) to any kind of real- and virtual environments from which it receives data for processing.

## 2.2 Installation and Compatibility

OpenViBE can be installed on computers running Windows XP or higher for both 32 and 64-Bit. However smooth running on 64-Bit architectures is not guaranteed as some drivers have yet to be included. It is advisable to use a 32-Bit system for example, if one intends to use the acquisition server for an online application.

To install the Software on Windows one needs to have the .NET framework (Microsoft Visual Studio 2008 or 2010) on their machines. The easiest way would be to download and run the installer (`win32-install_dependencies.exe`) directly.

OpenViBE also runs on Linux systems such as Ubuntu and Fedora, mainly the current versions. There is as yet no compatibility with the Mac OS architecture. Users having this platform would have to install a parallel Operating system like Windows or the Linux variants, which will probably impede efficiency as they can no longer make use of native UNIX capabilities.

Before one purchases any acquisition device one has to look under the list of supported hardware to verify compatibility of the acquisition server drivers with OpenViBE. The alternative would be to write one's own driver. However a good number of devices common on the market are supported.

## 2.3 User Modes

The platform has been designed for four different types of users. The developer and the application developer are both programmers; on the other hand the author and the operator do not need any programming skills.

**The Developer:** OpenViBE comes with a Software Development Toolkit (SDK) that enables the programmer to design, test and add new functionality to the platform. These could be on the Kernel or Plug-in basis.

**The Application Developer:** Uses the SDK to create standalone applications using OpenViBE as a library. Applications range from visual scenario editors to VR applications that the BCI user can interact with.

**The author:** (non-programmer) uses the visual scenario editor to arrange existing boxes to form a scenario. He configures these scenarios in order to create a compete ready-to-use BCI system. They however need knowledge of the internals of the platform as well as of BCI systems including basic signal processing.

**The Operator:** Also a non-programmer but with knowledge of neurophysiological signals, they would be generally a clinician or a practitioner. They simply run the pre-built scenarios of the author. Aided by visualization components, they are able to monitor the execution of the BCI.

**The User:** The user wears the acquisition gadget like the electrode cap and interacts with a BCI application by means of mental activity. The application could be a neurofeedback training program, a video game in virtual reality, a remote operation in augmented reality, etc. The user seldom directly uses the OpenViBE platform but rather they interact with it.

## 2.4 The architecture

The OpenViBE architectures, encapsulated in figure 2.1, is built around a kernel which employs a plug-in manager to ensure functional extensibility.

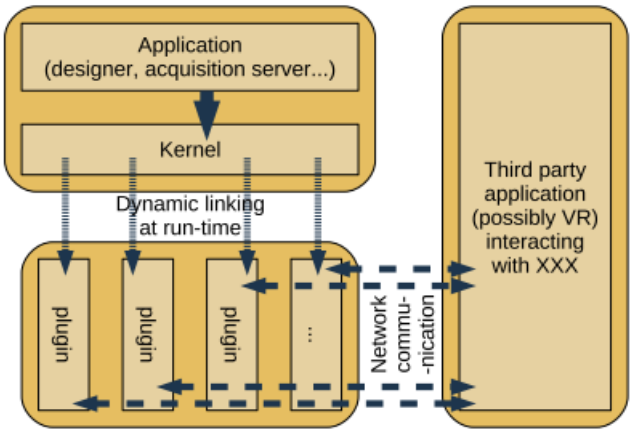


Figure 2.1: The OpenViBE software architecture [23]

The plug-in manager is able to dynamically load plug-in modules (e.g. DLL in Windows or .so files in Linux) and collect extensions from them. This allows for a quick and efficient expansion of functions and algorithms. Other managers around the kernel include:

- **Scenario manager** for creating and configuring scenarios: boxes can be added/ removed and configured to build a pipeline.
- **Visualization manager** for displaying graphical information. It relies on inbuilt libraries to render 2D and 3D graphical information in display windows.
- **Player manager** for runtime control over scenarios: It allows for playback, stopping, pausing and fast-forwarding.

## 2.5 Plug-ins

Three types of plug-ins are used:

1. The driver plug-in allows addition of acquisition devices to the acquisition server by using the SDKs or a physical connection.
2. Plug-ins for the algorithms allows developers to create and add new algorithms to the platform and encourages sharing and reuse of existing ones.
3. The box plug-ins generally rely on algorithm plug-ins to create different signal processing functionalities for the boxes. Among the boxes is one that accepts MATLAB code [23]. This is still under development by OpenViBE. Some boxes also support a scripting language called LUA for configuring the settings. These can be used for example to determine when to send stimulations in an application.

## 2.6 Tools

**The acquisition server** provides a generic interface to various kinds of acquisition devices e.g. EEG or EMG systems. Server connection to the hardware is dependent on manufacturers' specifications: some devices will be shipped with a specific SDK while others use a communication TCP/IP protocol over a network/serial/USB connection. Others will need proprietary acquisition software.

**The Designer** (Figure 2.2) is used mainly by the author and helps him to build complete scenarios based on existing software modules, using a dedicated graphical language and a simple GUI.

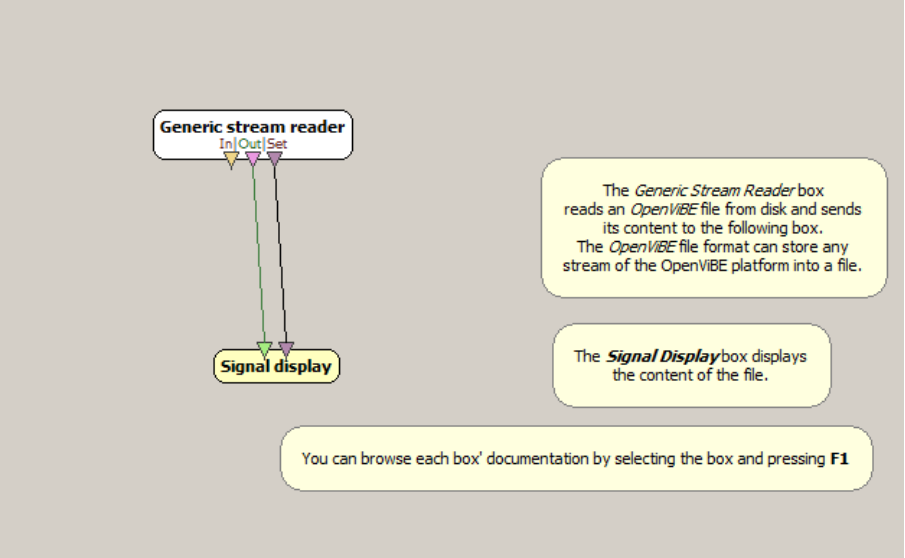


**Figure 2.2: The designer showing a simple scenario**

The tools enable the graphical design of a BCI system by adding and connecting boxes representing processing modules without writing a single line of code. The author has access to a list of existing modules in a panel and can drag and drop them in the scenario window. Each module appears as rectangular box with inputs (at the top) and outputs (at the bottom). The boxes are connectable through their inputs and outputs. Double clicking on a box shows its configuration panel. An

embedded player engine allows the author to test and debug their scenario in real-time.

## 2.7 Existing Scenarions and Tutorials

The platform comes with a number of ready-made scenarios to provide the uninitiated user with an overview of functionality, ranging from signal acquisition, analysis, visualization and rendering, through to complete BCIs that explore different aspects including integration with virtual reality. Relevant tutorials to some of these applications are also provided. There is clear in-scenario documentation as well as box documentation that can be accessed online. More information about these and new releases can be accessed on the OpenViBE website ( [6])

# 3 EEG Data Acquisition and Preprocessing

Acquiring a good EEG signal for use in developing a functional BCI requires knowledge of the physiological processes involved and factors that could influence the quality of signal attained; sources of errors and how to deal with them. Necessary hardware must however be in place. Of paramount importance is the ability to correctly interface the various components in order to acquire the signal, process it and build an application.

## 3.1 Hardware

For the experiments in this thesis the following hardware (Figure 3.1) was used:

1) A 32-Channel active electrode control box from *Brain Products* that comes with:
    - Electrodes (ch 1-32) and their connector
    - 2 extra electrodes (Ref and Gnd)
    - A 32-channel actiCAP standard 2, based on the 10-20 system
    - Active shielding from 50Hz power line interference
2) A TMSi Porti32 Refa: Amplifier (A/D converter) from *Twente Medical Systems International*, with the following specifications:
    - 24 unipolar recording ports
    - 4 bipolar recording ports
    - Digital ports
    - Sampling frequency of up to 2048 Hz/Channel
    - Fibre optic cabel for speedy data transfer to the computer (Bluetooth for wireless transfer)
3) Two DELL Optiplex 755 Desktop computers with :
    - Intel® Core™ 2 Duo CPU 2.66 GHz processor
    - 4.0 GB RAM
    - 32-Bit Windows Vista Service pac 2 Business
    - Both having OpenViBE and the actiCAP software installed.

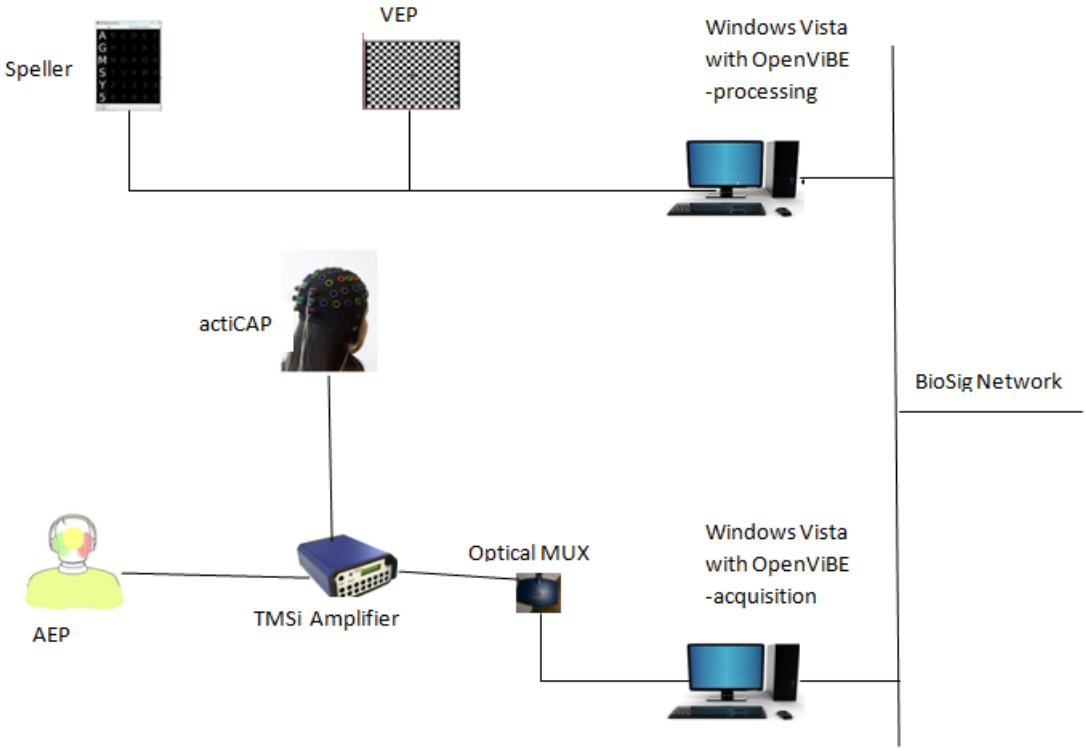


**Figure 3.1: Hardware layout for the experiments**[7]

When computers are used for recording EEG, the acquired analog signal has to be amplified since it is of very low amplitude, and digitized for further processing. Each channel is sampled repeatedly at a fixed time interval (sampling rate) and each sample is converted into its digital equivalent by the analog-to-digital converter (ADC). For quick and efficient streaming of these data samples to the computer, the TMSi Amplifier uses a bidirectional fiber optic cable instead of a wire connection. An inbuilt analog low pass filter tuned to a high sampling frequency is used as an anti-aliasing filter during signal acquisition. Digital low pass filters are then used to set the bandwidth of the acquired signal by eliminating frequencies outside the operating range.

[7] Sources: 1.Computer graphic from www.blogspot.de
2.Electrode cap graphic from www.brain-project.org
3. AEP graphic from www.clipart.com

## 3.2 Preparation and Interfacing

### 3.2.1 Dealing with Impedance

EEG has small amplitude (0.1 – 100 μV) because it undergoes attenuation through fluids, bone of the skull and skin before it can be picked up by the electrodes on the scalp. It is crucial that the recording gear helps to cleanly capture a quantity rather than distort it. High impedance may lead to distortions (artifacts) which can be difficult and costly to filter from the actual signal. The electrodes used with the actiCAP are Ag-AgCl disks (< 3 mm diameter) that are integrated with a tricolor LED system for showing the impedance of the skin-electrode interface. Embedded in the electrodes is an operational amplifier that acts as an impedance converter. Each electrode is connected with flexible leads to the TMSi amplifier through the router and control box as depicted in appendix A1(B). To achieve optimum recording, the electrode impedance has to be brought down to within 0 – 25 kΩ. After fitting the cap and the corresponding electrodes, before starting measurement, the control box is powered and the Z-button is pushed to start the impedance check-assisted by the actiCap software. The following color codes represent the three different classes of impedance levels:

- Green – Impedance  < 25 kΩ (optimum for acquisition)
- Yellow – Impedance 25 to 60 kΩ
- Red – Impedance > 60 kΩ

By applying a special conducting gel to the scalp using a syringe and needle, through the crevices on the electrode heads and gently massaging it in, the impedance is brought down to a working minimum (Appendix A1). This is indicated by transition of LED light from red; through yellow to green (It takes a while for the gel to act).

Depending on the number of electrodes involved, this process could take anywhere between 15 – 30 minutes. During signal acquisition Impedance check should be turned off but it is good practice to verify levels at the end of every measurement.

### 3.2.2 Connecting the Server and the Designer

The purpose of OpenViBE is to get data from the acquisition device through the acquisition server and send it to one or more clients for recording or processing [6]. In our experiments the client will be the OpenViBE designer, responsible for hosting the BCI application pipelines. As depicted in figure 3.2, the client(s) and server can run on the same machine or on different machines on a network. We use both interchangeably.

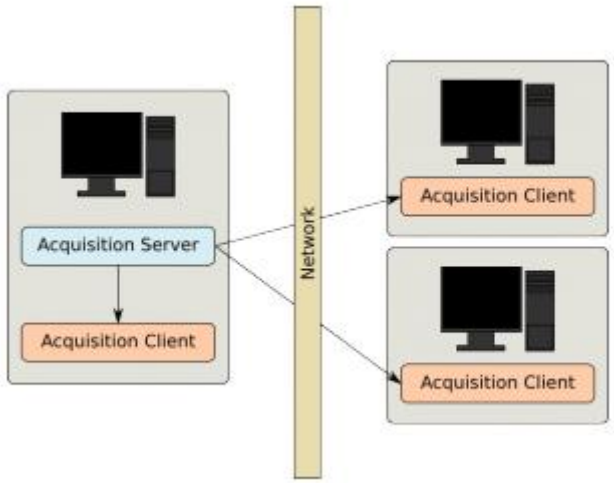


**Figure 3.2: Client server setup in OpenViBE [23]**

After starting the acquisition client, the acquisition driver matching the hardware type has to be selected in the drop down list. We chose *TMSi Refa32B*, matching our amplifier (figure 3.3). The *TMSi Refa32B* driver is still rather unstable and crushed on several occasions.

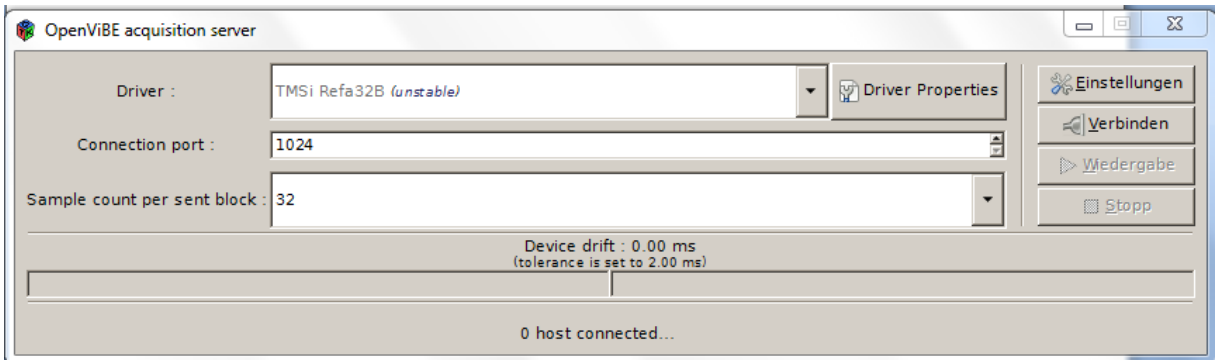


**Figure 3.3: Acquisition server interface. Hardware driver, number of electrodes and their names, sampling frequency and other settings can be done here**

### 3.2.3 Channel Selection and Naming

To get rid of unwanted noise in the signal, it is important that the number of channels be set to the number actually used in the acquisition (The default number is 32). Unused electrodes must also be decoupled from the amplifier. Appropriately naming the channels (Menus Driver properties and setting on the acquisition server) makes it easier for signal analysis and identification based on a given channel (Figure 3.3).

### 3.2.4 Sampling Frequency

An EEG signal as acquired by the electrodes from the scalp is an analogue quantity that needs to be digitized for further processing on a computerized system. The conversion is performed by means of the multichannel analogue-to-digital converter (ADC). The sample rate at which this is done must be enough to represent the change in the analog signal [24]. The effective bandwidth of the EEG signal is approximately 100 Hz. To satisfy the Nyquist criterion (equation 3), a minimum frequency of 200 Hz is recommended for sampling EEG signals in order to avoid distortions due to aliasing.

Mathematically, sampling is equivalent to multiplying the input analog signal with a series of Dirac-impulses:

$$y(t) = x(t) * \sum_{n=-\infty}^{\infty} \delta(t - nT_S) \qquad 1$$

Where $x(t)$ is the input signal, $y(t)$ the sampled signal, $\delta(t)$ a Dirac impulse and $T_S$ the period.

Multiplying the signals in the time domain amounts to a convolution in the frequency domain:

$$Y(f) = X(f) * \frac{1}{T_S} \sum_{n=-\infty}^{\infty} \delta\left(f - n\frac{1}{T_S}\right) = \frac{1}{T_S} \sum_{n=-\infty}^{\infty} X(f - n\frac{1}{T_S}) \qquad 2$$

There are periodicities in both time and frequency in the sampled signal, meaning that there should be symmetry or periodicity in the frequency domain to avoid overlaps [25], [26], [14], [27]. By the Nyquist criterion, the maximum frequency that can be sampled is half the maximum existing in the time domain. Thus:

$$T_S < \frac{1}{2\, f_{max}} \qquad 3$$

Failure to adhere to this condition results in a permanently distorted signal. However in a multichannel recording, setting the sampling frequency too high will lead to significant increase in memory use over time.

## 3.3 Artifacts in the EEG

### 3.3.1 Definition

Artifacts are unwanted components in a measured quantity that can be attributed to biological and technical processes involved in the measurement chain, that are not related to the physiological or pathological aspect of the point of measurement and its immediate surroundings. EEG signals must always be scanned for these distortions before they are processed for use in applications. The artifact in the recorded EEG may be either subject-related or technical. Subject-related artifacts are unwanted physiological signals that may significantly disturb the EEG. Technical artifacts include AC power line noise, electrode impedance, resistance in electrode

wires and other hardware specific noise. The most common EEG artifact sources can be classified in as follows:

Subject related:

- Artifacts related to minor body movements
- EMG
- ECG components (pulse, pacemaker)
- Eye movements (EOG)
- Sweat on the surface to be measured

Technical sources:

- 50/60 Hz power supply
- Impedance fluctuation
- DC components due to measurement electrodes
- Cable movements and broken wires [19]

Physiological artifacts can be minimized by introducing extra electrodes for ECG, EOG for example in the measurement. These can be subtracted out by the amplifier at the acquisition level. While impedance or resistance can be minimized and wires shortened, it is harder to eliminate noise caused by heating in the amplifier for example.

### 3.3.2 Filtering

Filters are applied in the frequency domain to eliminate unwanted components or features from incoming signals and to minimize artifacts. The attenuation of unwanted components might be partial or complete, depending on the choice of filter (settings). The aim of filtering should be to improve signal quality (gain) by minimizing background noise or interference. Filters do have one drawback however; they are usually associated with some loss of information and used wrongly, they could lead

to total loss of the signal. Two filtering techniques are employed; spatial and temporal filtering.

*Spatial filters:* combine data from two or more recording locations to derive features of a particular characteristic e.g frequency.

*Temporal filters:* employ a combination of frequency and amplitude restriction methods like band pass filtering (frequency) and Fourier analysis (amplitude) [7].

Some common filters in EEG signal processing are:

- Low pass filter – high frequencies are attenuated
- High pass filter – low frequencies are attenuated
- Band pass filter – passes in a given frequency range only
- Notch filter – rejects just one specific frequency (example of band pass)

### 3.3.3 Averaging

Averaging is done to enhance a time-locked signal component (like an evoked potential) in noisy measurements. Signal averaging in the time domain (spatial) assumes that:

1. Measured signal and noise are uncorrelated.
2. The timing of the signal is unknown.
3. A consistent signal component exists during measurement.
4. Noise in the signal is purely random with zero mean

For a measurement *x* consisting of signal *s* and noise *n* over N trials,

$$x_j(k) = s_j(k) + n_j(k) \qquad 4$$

represents the *kth* sample point in the *jth* trial.

The mean of the N sampled trials is given by:

$$\overline{x(k)_N} = \frac{1}{N}\sum_{j=1}^{N} x_j(k) = \frac{1}{N}\sum_{j=1}^{N}\left[s_j(k) + n_j(k)\right] \qquad 5$$

To reduce noise, we have to choose N large enough such that $x(k)_N \rightarrow s(k)_N$

From equation 3.5 we can derive the variance;

$$Var(\bar{x}) = \frac{\sigma_s^2 + \sigma_n^2}{N} \quad 6$$

Indicating that the estimate of s in the average $\bar{x}$ improves with a factor of $\frac{1}{\sqrt{N}}$ [24]

### 3.3.4 Signal to Noise Ratio

It is generally impossible to make a noise-free signal measurement: if the measurement chain is free of errors, some will be introduced by the instruments used (amplifiers, electrodes etc.). The aim of filtering is to make the noise component comparably small, relative to the signal component.

Signal-to-noise-ratio of a measurement;

$$SNR = 10 \log_{10} \frac{ms(signal)}{ms(noise)}\ dB \ = 20 \log_{10} \frac{rms(signal)}{rms(noise)}\ dB \quad 7$$

is the comparison of their power or amplitudes, where in discrete time series,

power is the mean squared amplitude :

$$ms = \frac{1}{N} \sum_{i=1}^{N} x_i^2 \quad 8$$

And amplitude is the root of the mean squared amplitude:

$$rms = \sqrt{\frac{1}{N} \sum_{i=1}^{N} x_i^2} \quad 9$$

For continuous time series,

$$ms = \frac{1}{T} \int_0^T x(t)^2\, dt \quad 10$$

$$rms = \sqrt{\frac{1}{T}\int_0^T x(t)^2\,dt} \qquad 11$$

A good measurement is one where SNR is high. This can be improved upon by signal processing. [24]. However if the power of the noise is greater than that of the signal, the noise will compete directly with the signal on the channel, resulting in reduction of the rate of data transfer or complete inability to read the signal.

## 3.4 Evoked Potentials

### 3.4.1 Definition and modalities

Evoked potentials (EPs), sometimes called Event Related Potentials (ERPs), are low amplitude (0.1 to 10 μV) transient waveforms that appear in the ongoing background EEG as a (exogenous) response to an external stimulus the user was given. They are electrical responses in the brain (cortex) or the brainstem to various types of sensory stimulation of nervous tissues [5] therefore they tend to have a latency related to the time of stimulation presentation. Their amplitude is the sum of a large number of action potentials (APs) that are time locked to sensory, motor or cognitive events [14]

**Auditory Evoked Potentials (AEP):** are generated in response to an auditory stimulus usually produced by a short sound wave. AEPs give an insight into the propagation of neural information by the acoustic nerve from the ear to the cortex and can be used to diagnose ailments and complications to this pathway, including hearing loss.

**Visual Evoked Potentials (VEP):** There are two common methods for eliciting VEPs; in one the stimulus is given as a pattern reversal, for example alternating black and white squares of a chess board on a monitor display. The other stimulus is given as flashing sequences (see 4.3.1). The electrical response elicited by visual stimuli can be recorded from the scalp in the occipital region of the brain (Figure 1.7) and can serve as an evaluation for visual pathway functionality and diagnosis of ocular and retinal disorders.

**Somatosensory Evoked Potentials (SEP):** Elicited by electrical stimulation of peripheral nerves from the surface of the body, this type of EPs can offer valuable information about nerve conduction and the functionality between selected stimulation points from the spinal cord through to the cerebral cortex. It is a method of intraoperative monitoring during spinal cord surgery [5].

Measured amplitude of the EPs usually depends on the type and strength of the stimulus, electrode position on the scalp, including mental state of the user; i.e. varying degrees of attention and wakefulness. Commonly used in BCIs applications are auditory and visual stimulation, where the most common evoked potential used is the P300. EPs can also be elicited as a response to performing cognitive functions such those that require attention and memory processes. These responses are termed endogenous since they do not involve physical stimuli.

### 3.4.2 Noise and EPs

The recorded EEG contains P300 potentials as well as other brain activities, muscular and or ocular artifacts leading to a very low signal-to-noise ratio (SNR) of the P300 potential [28]. These brain activities are unrelated to the experiment and produce waves with higher frequency bands in comparison to the evoked potentials. The frequency content of muscular (movement) artifacts can usually not be removed by low-pass filtering. Further, the frequencies of the background EEG overlap (harmonics) with the evoked potentials such that conventional filtering cannot be used to achieve higher SNR [29]. To cancel out the noise, epochs of the evoked potential have to be averaged (see 3.3.3). Sampling more epochs improves SNR.

# 4 Experiments and Results

## 4.1 The P300 Speller

### 4.1.1 Experiment in brief

The experiment is based on the “odd-ball” paradigm first developed by Farwell and Donchin (1988) and analyzed in [30] It utilizes the P300 event related potential (ERP) elicited by instructing a subject to focus on a character contained in a 6x6 grid of alpha-numeric characters; A-Z and 0-9 (Figure 4.1).The computer generates flashing sequences of rows and columns at a preset frequency (visual stimuli). The user is asked to distinguish between a common stimulus (non-target) and a rare stimulus (target) [28]. This can be done for example by mentally counting up each time the target flashes in a row or in a column and ignoring the non-targets. It is odd-ball because the events on which it depends can be classified into two categories, where one of them, the target event, is rarely presented. Also the task to be performed depends on these two events. The rare event elicits an ERP with a P300 component. Since the events are mixed, determining wanted results is purely statistical and is dependent on a classifier algorithm. On average nearly 20% of all flashes will contain the target character and the other 80% will not [5]. Theoretically, by determining which rows and columns elicited an ERP and further determining their intersection (cell), the computer is able to predict the character the user was focusing on. However the recorded EEG contains elicited ERPs as well as other brain activities (noise) including artifacts due to involuntary blinking, decreasing the signal-to-noise ratio (SNR) of the P300 waves. According to Donchin [30], increasing classification accuracy is done by averaging epochs over repeated trials. Many repetitions decrease the number of characters/minute the user can spell however. The xDAWN algorithm employs a Bayesian linear discriminant analysis to synchronize target stimuli with the evoked potentials and uses spatial filtering to enhance their power thereby increasing efficiency of classification. More on this in Rivet et al [28].

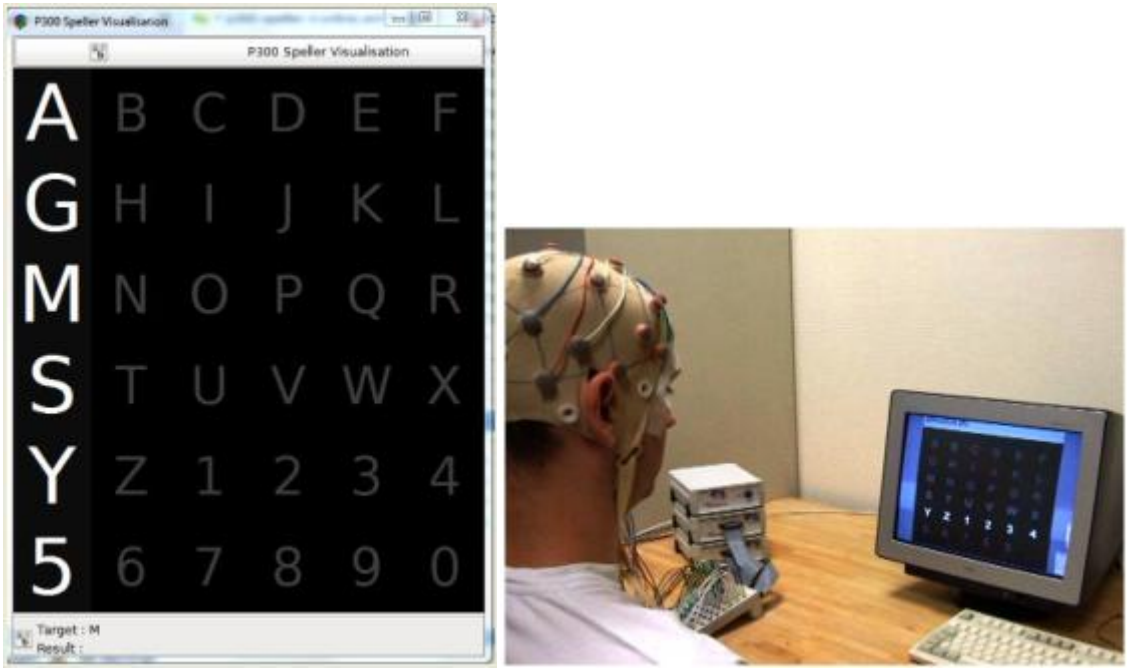


**Figure 4.1: The alphanumeric grid and visual stimulus; the subject focuses on a character [23]**

### 4.1.2 Method

A black box test was carried out using an existing xDAWN P300 speller in OpenViBE. The experiment sought to reproduce the described results of the BCI using our acquisition hardware. This BCI is divided into four scenarios:

1. Data acquisition
2. xDAWN spatial filter training
3. P300 classifier training
4. Online use of the speller

The experiment involved 5 able-bodied subjects (users) with no prior experience at the start: 4 male and 1 female, all above 18 years of age. All but the female subject repeated the experiment at least once on different days. Subjects were seated comfortably in a quiet with minimum illumination, at a distance approx. 1m away from the monitor.

**Step1** *Acquiring data:* After a background signal check, recording was done using the actiCAP and with 16 Ag-AgCl unipolar electrodes ($FP_1$, $FP_2$, $F_3$, $F_z$, $F_4$, $C_3$, $C_z$, $C_4$, $P_7$, $P_3$, $P_z$, $P_4$, $P_8$, $O_1$, $O_z$, $O_2$) whose impedance levels were brought to within (0 -25 kΩ)

– green (section 3.2.1). The cap has no *Nasion* electrode but offers in its place a *Reference* electrode. The signals were amplified and digitized using a grounded TMSi amplifier (see Hardware) at the OpenViBE default rate of 512 Hz and a sample count of 32 per block, delivering 512/32 = 16 blocks of data per second. We used one computer as the server and the other as the client on a network. In this session the subject is asked to focus on the character suggested by the computer (highlighted by blue) on the 6x6 grid (figure 4.1). They were further instructed to mentally count the number of times this character is intensified in a randomly flashing row or column. A total of 10 trials (number of characters) are done in each session. Each row/column is intensified for a duration of 100 ms (0.1 sec) with an interval of 50 ms from one flash to the next. There are 12 flashes of each row and 12 of each column on the grid, so each character is intensified 24 times during every trial. From one trial to the next, there's a delay of 4 seconds to allow the user to change focus on the next character. In the scenario, this is timed at about 30 seconds from the onset of one character to the next, translating to ca. 5 minutes for the entire session of 10 trials. The data was stored in signals folder (*ov format) with a time stamp.

**Step 2** *Preprocessing and training:* The recorded data file in step 1 is read with a generic stream reader. A $4^{th}$ order Butterworth band-pass filter (1.0 – 20.0 Hz) was used to filter out unwanted signals components. Signal decimation is then used to cut a 1 second block of 16 samples into four blocks of 4 samples each. The blocks are sampled again in epochs of 250 ms each.

Spatial filtering is then done using the xDAWN filter that reduces the signal space to 3 dimensions, most significant for detecting a P300 ERP [23]. This is the offline training of the filter.

**Step 3** *Training the LDA classifier*: In scenario 3 again the raw data file is read with the stream reader and fed into the one hand into the preprocessing pipeline and xDAWN spatial filter which has been trained in step 2, on the other hand nothing is done to the raw signal. Both signals are then fed into separate stimulus based epoching boxes set at duration of 600 ms each. The boxes synchronize the ERPs with the target event and the rest of the signal with the non-target event. The averages of these two blocks are computed every second, aggregated and used to train the linear discriminant algorithm of the classifier. The classifier should now be

able to detect a p300 (target) waves and discriminate it from the background (non-target) waves.

**Step 4** *Using the Speller online*: Having trained the spatial filter and the classifier, a new signal was recorded for an online session: It was preprocessed in the same pipeline as in step 2. The output of the xDAWN filter was passed to 12 separate but identical pipelines, one for each repetition of row/column (step 3 above). At the end of the pipeline is a classifier (LDA) which after calibration, passes the output to a voting classifier, configured (default) to reject non-target input and pass the target character to the P300 speller visualization for rendering on the grid. A target character is intensified in green (Figure 4.2 below). This would be the character the algorithms have predicted as intended input from the user and is displayed as the result for each of the 10trials

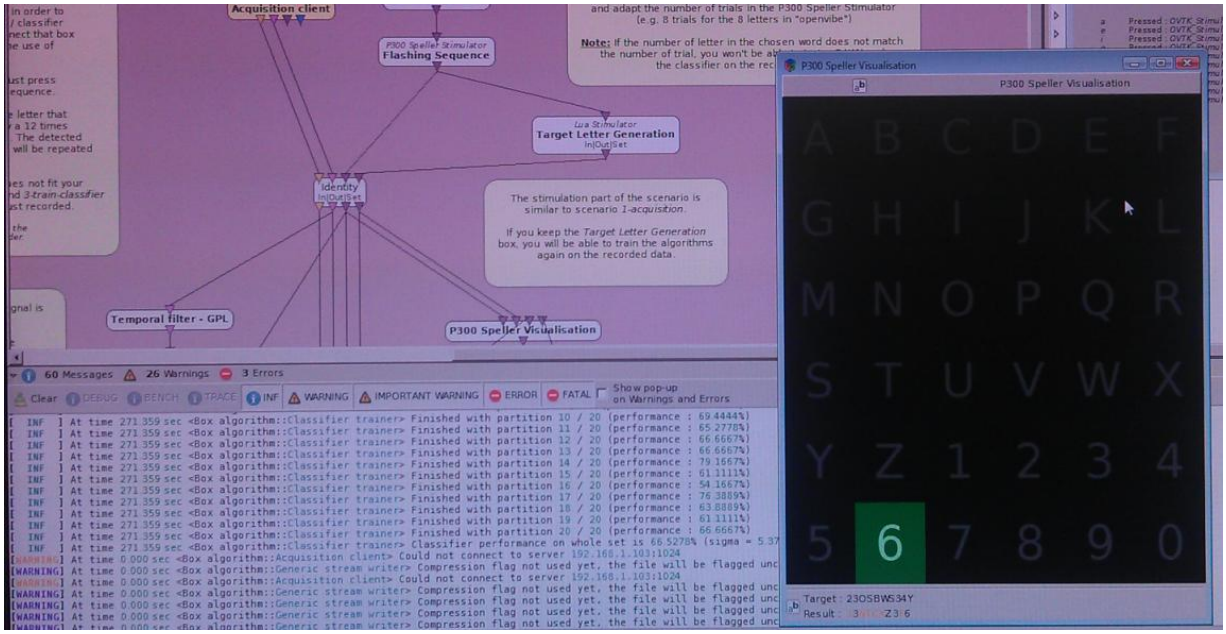


**Figure 4.2: A typical output from the P300 speller application in the online session**

After a trial the target character chosen by the classifier algorithms is highlighted in green. At the end of the spelling session there are two rows at the bottom of the grid:

1. Target for the characters suggested by the computer and,

2. Result for the characters the algorithms identified as input from the user. To the left, the console output as classifier performance on each of the used electrodes including the mean and standard deviation.

### 4.1.3 Performance

The following performance values were observed for the five subjects in both the offline classifier training and the online trial with the speller.

**Table 2: Results of the experiment involving 5 subjects**

| Subject | Average Classifier Performance (%) | Number of Characters correct out of ten |
|---|---|---|
| A | 66.52 | 2/10 |
| B | 68.26 | 1/10 |
| C (Female) | 75.34 | 1/10 |
| D | 77.45 | 0/10 |
| E | 67.69 | 1/10 |

The results depicted were all obtained with the default settings in the OpenViBE scenarios for the xDAWN speller. The documentation of the scenarios suggested that a performance of the classifier above 70% would be necessary for the user to achieve at least 80% score in the online session. Subject A's classifier result is below the required result in comparison to Subject D's 77.5% that is several points above. However D achieves no score on the speller to A's 2/10.The average score of 1/10

on the speller for all the participants is clearly very low and seems to suggest a randomness of result, rather than a correct performance of the classifier on target/non-target discrimination.

### 4.1.4 Problems and Mitigation

The failure to achieve satisfactory results could not be directly attributed to any one factor. The obvious exclusion here is subject related failure, as performance was poor for all of them. From hardware, to acquisition and settings in the algorithms of different pipelines in the scenarios, any of these could be the problem. It could well be the software platform itself.

A first approach to validating the results was to try and adjust the speed of the row/column flashes in both the acquisition and online scenarios to find out whether it improved the subjects' score on the speller: it was suspected that perhaps the rate of repetition, at 150 ms, was too fast, leading to an interference of the P300 response wave and the following stimulus. For two of the subjects, one male (B) and the female (C), the experiment was repeated with the flash duration set to 400 ms (Figure 4.3) making an inter repetition delay of 450 ms, a 200% slow down. The graphics in figure 4.4 show the obtained classifier performances.

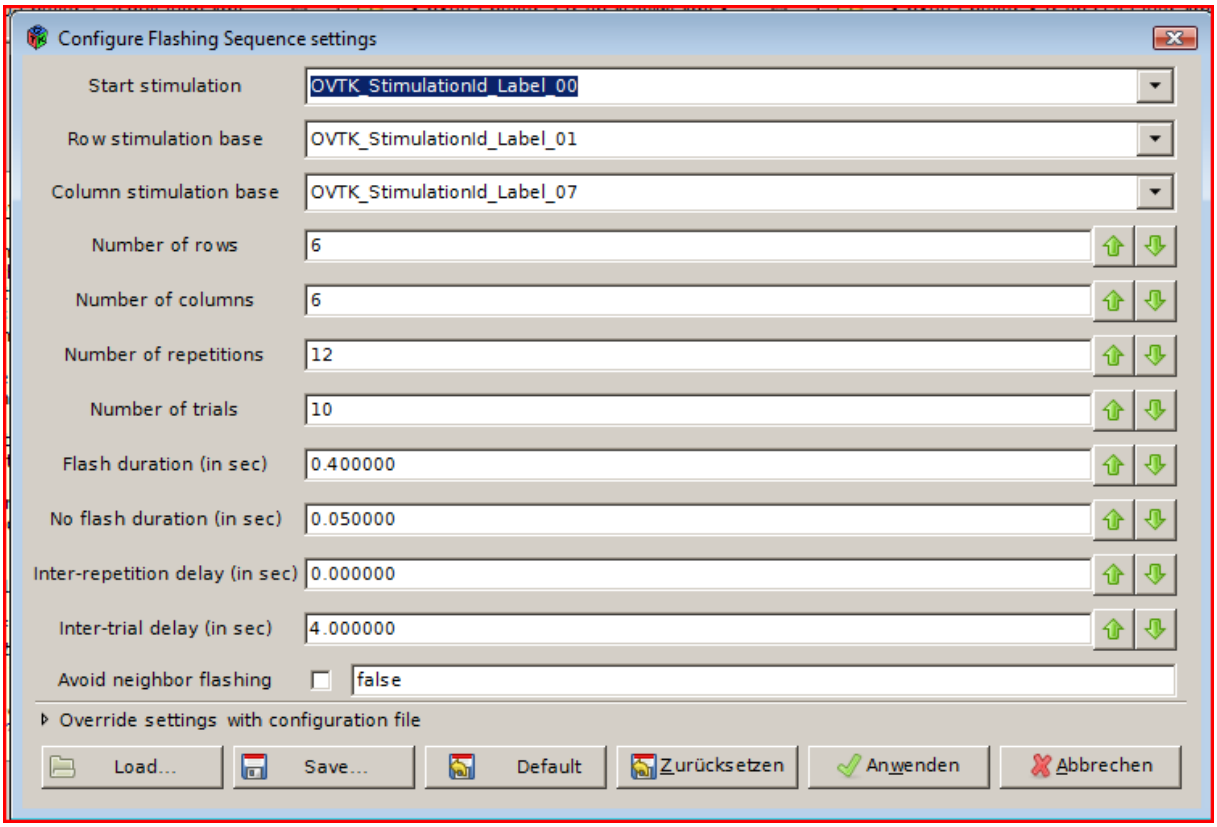


**Figure 4.3: Flash duration in the flashing sequence settings changed from 100 to 400 milliseconds**

Subject B

```
[  INF  ] At time 697.117 sec <Box algorithm::Classifier trainer> Finished with partition 13 / 20 (performance : 84.7222%)
[  INF  ] At time 697.117 sec <Box algorithm::Classifier trainer> Finished with partition 14 / 20 (performance : 73.6111%)
[  INF  ] At time 697.117 sec <Box algorithm::Classifier trainer> Finished with partition 15 / 20 (performance : 70.8333%)
[  INF  ] At time 697.117 sec <Box algorithm::Classifier trainer> Finished with partition 16 / 20 (performance : 76.3889%)
[  INF  ] At time 697.117 sec <Box algorithm::Classifier trainer> Finished with partition 17 / 20 (performance : 68.0556%)
[  INF  ] At time 697.117 sec <Box algorithm::Classifier trainer> Finished with partition 18 / 20 (performance : 68.0556%)
[  INF  ] At time 697.117 sec <Box algorithm::Classifier trainer> Finished with partition 19 / 20 (performance : 80.5556%)
[  INF  ] At time 697.117 sec <Box algorithm::Classifier trainer> Finished with partition 20 / 20 (performance : 79.1667%)
[  INF  ] At time 697.117 sec <Box algorithm::Classifier trainer> Classifier performance on whole set is 75.4861% (sigma = 4.54901%)
```

Subject C

```
[  INF  ] At time 422.180 sec <Box algorithm::Classifier trainer> Finished with partition 6 / 20 (performance : 81.9444%)
[  INF  ] At time 422.180 sec <Box algorithm::Classifier trainer> Finished with partition 7 / 20 (performance : 84.7222%)
[  INF  ] At time 422.180 sec <Box algorithm::Classifier trainer> Finished with partition 8 / 20 (performance : 84.7222%)
[  INF  ] At time 422.180 sec <Box algorithm::Classifier trainer> Finished with partition 9 / 20 (performance : 77.7778%)
[  INF  ] At time 422.180 sec <Box algorithm::Classifier trainer> Finished with partition 10 / 20 (performance : 83.3333%)
[  INF  ] At time 422.180 sec <Box algorithm::Classifier trainer> Finished with partition 11 / 20 (performance : 77.7778%)
[  INF  ] At time 422.180 sec <Box algorithm::Classifier trainer> Finished with partition 12 / 20 (performance : 79.1667%)
[  INF  ] At time 422.180 sec <Box algorithm::Classifier trainer> Finished with partition 13 / 20 (performance : 83.3333%)
[  INF  ] At time 422.180 sec <Box algorithm::Classifier trainer> Finished with partition 14 / 20 (performance : 91.6667%)
[  INF  ] At time 422.180 sec <Box algorithm::Classifier trainer> Finished with partition 15 / 20 (performance : 80.5556%)
[  INF  ] At time 422.180 sec <Box algorithm::Classifier trainer> Finished with partition 16 / 20 (performance : 90.2778%)
[  INF  ] At time 422.180 sec <Box algorithm::Classifier trainer> Finished with partition 17 / 20 (performance : 83.3333%)
[  INF  ] At time 422.180 sec <Box algorithm::Classifier trainer> Finished with partition 18 / 20 (performance : 79.1667%)
[  INF  ] At time 422.180 sec <Box algorithm::Classifier trainer> Finished with partition 19 / 20 (performance : 86.1111%)
[  INF  ] At time 422.180 sec <Box algorithm::Classifier trainer> Finished with partition 20 / 20 (performance : 81.9444%)
[  INF  ] At time 422.180 sec <Box algorithm::Classifier trainer> Classifier performance on whole set is 84.0278% (sigma = 4.35899%)
```

**Figure 4.4: Console Information from classifier performances of subject B (75.49%) and subject C (84.03%) with the inter-repetition duration of 450 milliseconds**

Clearly there was a marked improvement in the classifier performance: 9.6% and 8.7% for B and C respectively. However they both had a 0/10 score in the online spelling session. This is counterintuitive because the classifier seems to have identified the evoked potentials correctly.

### 4.1.5 Inference

While the results above indicate that slowing inter-repetition improves on classifier performance, a corresponding improvement on the score in the online sessions was not registered. It is probable that the output numbers of the classifier are misleading: that it has failed to discriminate the P300 components from the ongoing EEG signal therefore there's no clear distinction of target and non-target stimuli. It has to be noted that evoked potentials are transient in nature and are in order of magnitude 10 times smaller than the ongoing background EEG. In this case the EEG would be a noise masking the EPs, which the spatial filters have to actively eliminate. If the algorithms (Spatial filter, LDA-classifier) are working well, it could be that the signal is leaking at some unknown point. Furthermore the speed of data transfer on the network is unknown and the latency of triggers for the stimuli may not be synchronized.

## 4.2 Visualizing Evoked Potentials

We consider the visualization of evoked potentials as validation for the proper functioning of the acquisition apparatus and the software platform. We seek to establish existence of the P300 EPs in the ongoing background EEG, which potentials are crucial to the success of P300 speller BCI application.

### 4.2.1 Visual Evoked Potentials

The experiment was set up using pattern reversal of a chessboard graphic displayed on a monitor as the stimulus (Figure 4.5).The subject was instructed to focus on the center as the squares alternately changed color between black and white. There was

minimal ambient light with the interstimulation interval set to 2 seconds in the LUA script. Using the actiCap, the subject's EEG was recorded with electrodes ( $P_z$, $O_1$, $O_2$) placed in the region of the visual cortex (Figure 1.7). $C_z$ was used as a reference electrode. The recorded signal was analyzed in MATLAB for the transient P300 peaks.

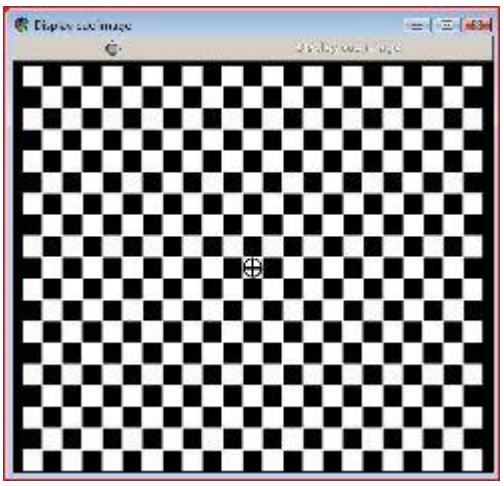

**Figure 4.5: Visual stimulus, constantly timed pattern reversal as seen by subject**

According to Sörmno & Laguna [5], a normal subject's VEP waveform is described by a small positive peak, a larger positive peak occurring about 75 ms after stimulus (N75), and a large positive peak about 100 ms after stimulus (P100). The duration of the VEP may extend beyond 300 ms. In figures 4.6 and 4.7 we observe all these three characteristics, which is proof that the hardware used and the software platform are capable of reproducing an expected response potential.

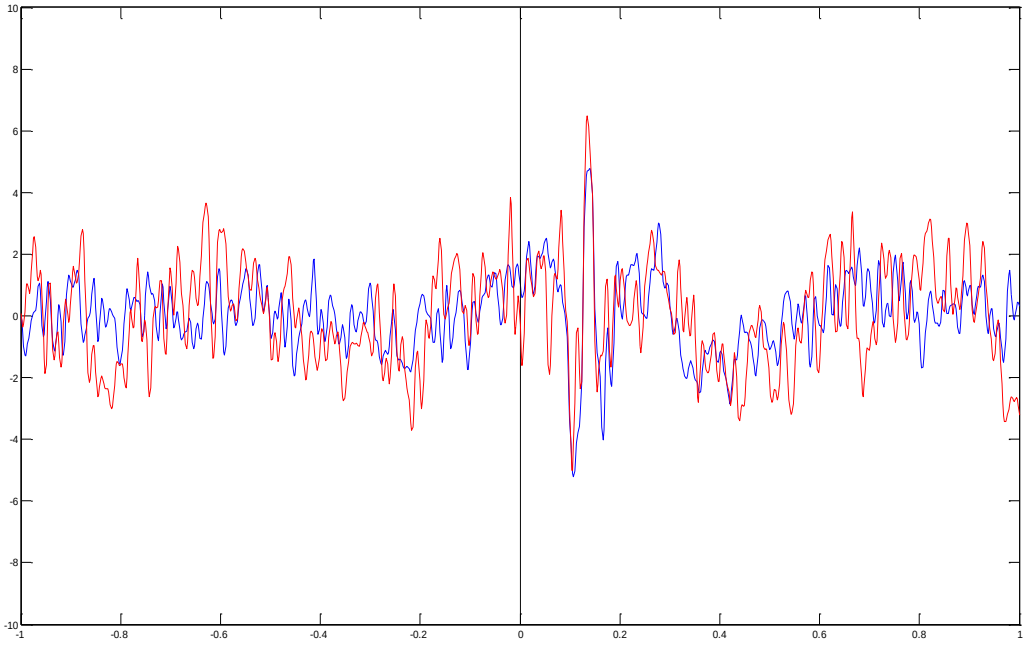


**Figure 4.6: Red is average over background EEG, blue is average over rare potential**

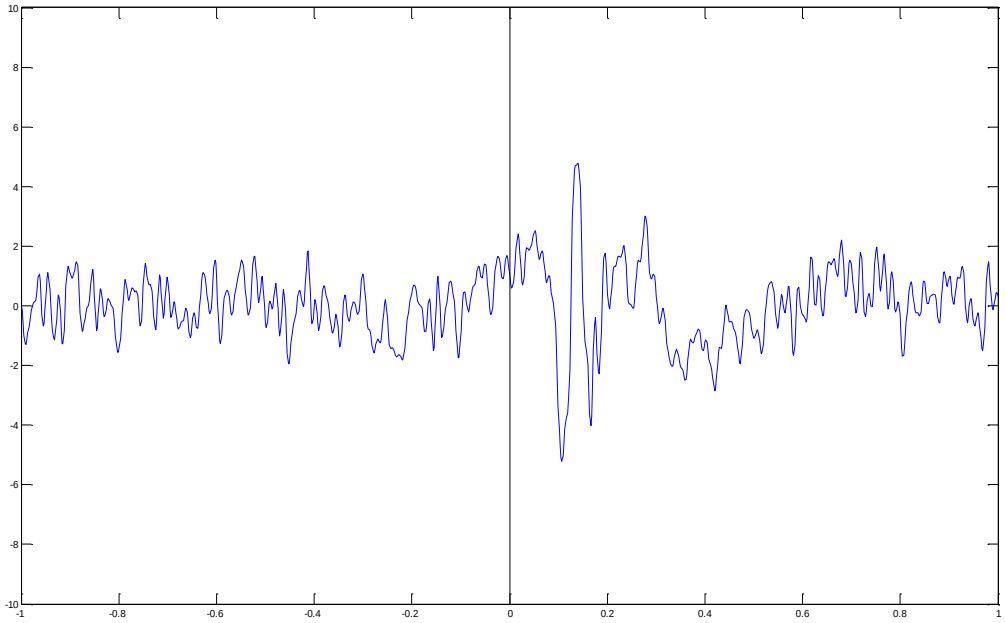


**Figure 4.7: Characteristic P300 peak in 200 - 400 ms range**

### 4.2.2 Auditory Evoked Potentials

In this experiment the subject wore a set of stereo headphones. With his eyes closed, he was instructed to concentrate and mentally register the occurrence of a rare high frequency ton, the target stimulus, and ignore the normal low frequency ton, the non-target. 2000Hz was used for the target and 1000 Hz for the non-target. The subject's EEG was recorded with the same electrode placement as in 4.2.1 above and the signals analyzed in MATLAB.

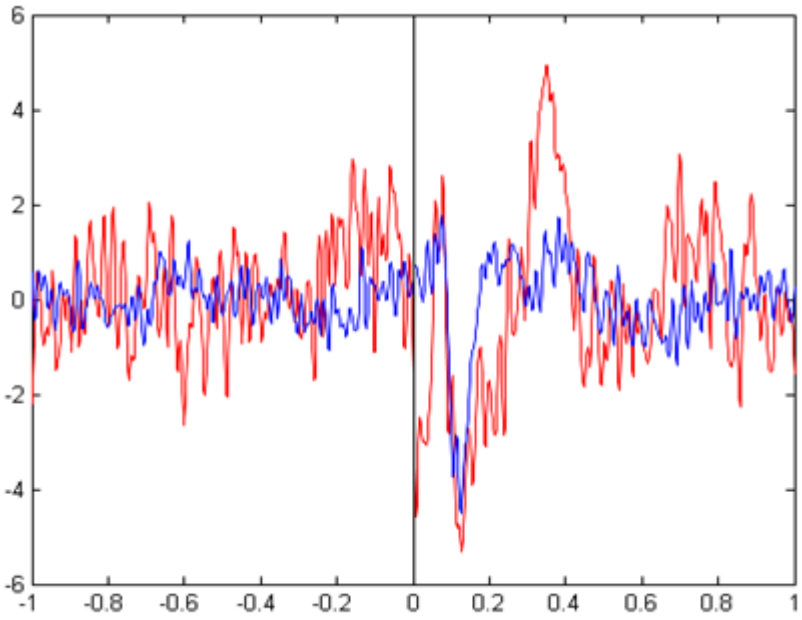


**Figure 4.8: High pass filtered (1 Hz on Cz - Pz). Red is target and blue non-target**

A normal AEP shows marked difference in signal properties, relating to the various structures located in the auditory pathway. Figures 4.8 and 4.9 show the P300 wave as a response to the target stimulus and the normal wave train for the non-target.

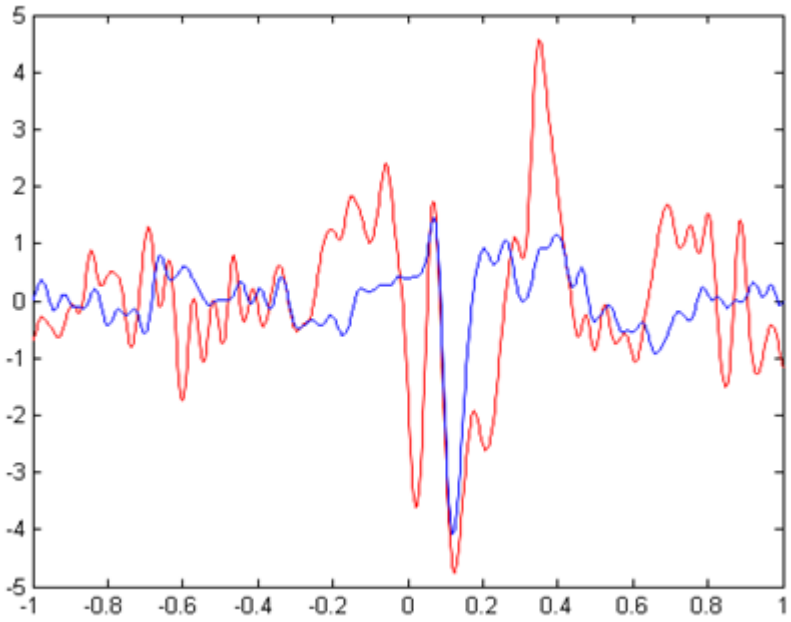


**Figure 4.9: Band pass filtered (1 - 70 Hz on Cz-Pz). Red is target, blue non-target**

## 4.3 Investigating Latencies

We use two sinus wave audio signals, 200 Hz (target) and 100 Hz (non-target) in a scenario with two signal generators and stimulation to record and analyze the time dependencies in OpenViBE. 2 minutes of the signal was recorded at a sampling rate of 2048 Hz, with two variations:

1. Unipolar recording (2 electrodes with 1 ground)
2. Bipolar (1 bipolar pin with 1 ground)

A visual inspection of the acquired signal in OpenViBE (Figure 4.10) indicates a delay of about 0.2 seconds of the signal on the stimulation. Also, malformation of the wave suggests a signal leak in the amplifier or, more likely, a loss of samples during transmission over the TCP/IP protocol on the network. Another possibility is a replacement of missing samples by the OpenViBE-TMSi acquisition server.

**Figure 4.10: Display of acquired bipolar audio signal in OpenViBE indicating latency and distortion**

We further analyzed the bipolar recording in matlab.

Arrival of first epoch (8438/2048) = 4.1201 seconds

Arrival of first stimulation = 4.0547 seconds

**Table 3: Bipolar AEP recording on network (1 client, 1 server)**

| Signal time (s) | Stimulus time (s) | Delay (ms) |
|---|---|---|
| 4.1201 | 4.0547 | 65.4 |
| 7.1128 | 7.0547 | 58.1 |
| 10.1196 | 10.0547 | 64.9 |
| 16.1162 | 16.0547 | 61.5 |
| 19.1191 | 19.0547 | 64.5 |

*Mean delay = 62.88 ms*

*Standard deviation = 3.07 ms*

*Latency = 62.88 ± 3.07 ms*

**Table 4: Bipolar AEP recording on same computer (client same as server)**

| Signal time (s) | Stimulus time(s) | Delay (ms) |
|---|---|---|
| 4.1064 | 4.0547 | 51.7 |
| 7.1079 | 7.0547 | 53.2 |
| 10.1074 | 10.0547 | 52.7 |
| 16.1035 | 16.0547 | 48.8 |
| 19.1074 | 19.0547 | 52.7 |

*Mean delay = 51.82 ms*

*Standard deviation = 1.77 ms*

*Latency = 51.82 ±1.77 ms*

These results suggest that for the Bipolar recording, the network connection slows down the signal by a minimum of 11 milliseconds. Moreover, the transport across the network between two different computers appears to increase the standard deviation of the latencies.

**Table 5: Unipolar AEP recording on network**

| Signal time (s) | Stimulus time (s) | Delay (ms) |
|---|---|---|
| 4.1147 | 4.0547 | 60.00 |
| 7.1162 | 7.0547 | 61.50 |
| 10.1147 | 10.0547 | 60.00 |
| 16.1172 | 16.0547 | 62.50 |
| 19.1113 | 19.0547 | 56.60 |

*Mean delay = 60.12 ms*

*Standard deviation = 2.24 ms*

*Latency = 60.12 ± 2.24 ms*

**Table 6: Unipolar AEP recording on same computer (client same as server)**

| Signal time (s) | Stimulus time (s) | Delay (ms) |
|---|---|---|
| 4.1016 | 4.0547 | 46.9 |
| 7.1011 | 7.0547 | 46.4 |
| 10.1220 | 10.0547 | 67.3 |
| 16.1000 | 16.0547 | 45.3 |
| 19.1001 | 19.0547 | 45.4 |

We ignore the runaway value in row 3 to achieve:

*Mean delay = 46.00 ms*

*Standard deviation = 0.79 ms*

*Latency = 46 ± 0.79 ms*

We can infer that the unipolar signal is at least 14 ms faster on a same computer recording as compared to the network setup.

Without analyzing hardware and software performance in these experiments, we can generally conclude from the results of tables 2, 3, 4 and 5 that signal acquisition will always have a time delay. It is also clear that unipolar recording delivers the signal faster than the bipolar recording and on the whole, network acquisition is slower than acquisition on the same computer. The smaller standard deviation values also indicate that the timing of the signals and stimuli is more exact compared to network acquisition.

How latency affects performance of a particular BCI application like the visual speller and what magnitudes would be admissible is not yet clear. Eliminating latency does not guarantee good performance however. According to Cecotti & Gräser [31], reducing BCI latency typically impairs accuracy. There has to exist a compromise between speed and accuracy.

# 5 Discussion of Results

The aim of this thesis was to use the acquisition hardware available in the BioSig laboratory at Hochschule Heilbronn, to reproduce a P300 visual speller on an open source software platform. From the many freely available platforms, FieldTrip and OpenViBE were singled out because of their modularity approach, providing ready to use tools and algorithms. FieldTrip is a Matlab based Toolbox for EEG/EMG analysis that includes no graphical interface; therefore it relies on the Matlab console and still requires a good understanding of this programming language. OpenViBE on the other hand has an integrated graphical interface and uses a more simplified graphical language to enable the user to prepare pipelines for signal processing, visualization and applications like BCIs, without having to write any line of code (see chapter 2). Work started with an analysis of both platforms at the end of which OpenViBE was chosen. This was followed by a literature review, to get acquainted with the many aspects of brain computer interfaces, including signal processing, neuroscience and the EEG, human computer interaction and assisted living for the disabled.

The approach taken in this thesis was not do develop an own visual speller but rather recreate an off-the shelf application from OpenViBE with the kind of hardware we had in the laboratory. On account of the results as indicated in (4.3 - 4.5) this experiment was not a success and the aim of the thesis was in part not achieved. On the other hand, invaluable insight was gained, through research, into the technical aspect of a brain computer interface. This has been documented in this thesis and it is hoped that it will provide a good basis for future works on this topic. The reason(s) for failure to produce satisfactory results in this experiment are yet unknown but a few can be singled out for future reference: The speller application involves four separate scenarios (see 4.1.2), each with its own characteristic pipeline and settings for boxes and algorithms. For the most part, we used these unchanged: It is likely that a few alterations could lead to better results but it also difficult to assess which part of the pipeline works well and which doesn't. There was the question of loss of signal by the amplifier as evidenced by the sine waves in OpenViBE (figure 4.9) and further observed during analysis of the signal in MATLAB. We did not compare input to output results of the amplifier and where the inbuilt analog and digital filters were working well so it is unclear whether this was a contributing factor. We were able to

establish the existence of typical transient evoked potentials synchronized with their target stimuli (see 4.2.1) however the classifier algorithm in the online scenario did not identify these correctly. It is probable that the xDAWN spatial filter did not narrow down the space, to enhance the accuracy of the classifier algorithm. Accuracy of the classifier depends heavily on the signal-to-noise ratio of the evoked potentials so if the filters do not perform optimally, the classifiers will also falter. According to Bießmann [32], shortening inter stimulus interval (ISI) does not adversely affect the accuracy of the classifier. We used an ISI of 150ms (default setting) of which 50ms was no flash duration. Slowing down the flash duration three-fold to achieve ISI of 450 ms improved the classifier performance but not that of the speller with the two subjects, as can be seen from the results (see 4.1.4). Latency in the acquired signal would seem to suggest that the evoked potentials are not synchronized with the stimuli therefore leading to improper classification. But the P300 wave has a latency of about 600ms and the highest recorded latency on our system was about 63ms which would shift the center of the wave from 300 to about 360 – 400 ms, which is within range.

On evidence of the visualization experiments in 4.2.1 we can conclude that the hardware and the software platform together can be used to acquire a good EEG signal. It also has to be noted that visualization of the EPs in OpenViBE could not be achieved, hence the migration to MATLAB. On the flipside, OpenViBE will soon fully support MATLAB scripting, making it possible to replace some of the boxes in the pipelines with own algorithms.

# 6 Outlook

Unsatisfactory results recorded in the visual speller notwithstanding, this thesis has undoubtedly covered aspects of the BCIs that will be of help to others researching this topic in the future. Basing on the results of the experiment it can be suggested that realizing an own spatial filter and classifier especially with a high level language like MATLAB, which in the future will be fully supported by the OpenViBE platform, with the added advantage of the LUA scripting language, could be the way to achieving better.

Brain computer interfaces are a novel way to give disabled people and locked in patients the means to live a comparably normal life again. However the rates of data transfer in current applications is still very low; about 25 bits/minute according to Walpow [7] therefore they are only capable of basic communication and control functions. Visual spellers have been documented to achieve only 2-3 words per minute. With ever increasing computing power, transfer rates of the BCIs will also improve. For now word prediction algorithms like those used in phone messaging could be integrated to achieve a higher spelling rate on lower processing power.

## Bibliography


[1] D. S. Tan, "Brain-Computer Interfaces : Applying our Minds to Human-Computer Interaction," Springer-Verlag London Limited, London, 2010.

[2] Microsoft Corporation, "Being Human, Human-Computer Interaction In The Year 2020," Microsoft Research Ltd, Cambridge, 2008.

[3] F. Walsh, "BBC News Health," 16 May 2012. [Online]. Available: http://www.bbc.co.uk/news/health-18092653. [Accessed 28 June 2012].

[4] TedGlobal, Director, *A Headset tha reads your brainswaves.* [Film]. 2010.

[5] L. Sörnmo and P. Laguna, Biolectrical Signal Processing in Cardiac and Neuronal Applications, Massachussetts: Elsevier Academic Press, 2005.

[6] Inria Rennes (2012), "Open Vibe," 04 2012. [Online]. Available: http://openvibe.inria.fr/.

[7] J. R. Wolpaw, N. Birbaumer, D. J. McFarland, G. Pfurtscheller and T. M. Vaughan, "Brain-Computer Interfaces for communication and Control," *Clinical Neurophysiology,* no. 113, pp. 767-791, 2002.

[8] E. N. Bruce, Biomedical Signal Processing and Signal Modeling, New York: John Wiley & Sons, Inc, 2001.

[9] N. Birbaumer and L. G. Cohen, "Brain Computer Interfaces:Communication and Restoration of Movement in Paralysis," *The Journal of Physiology,* 2007.

[10] M. Kurz, W. Almer and F. Landolt, "Brain Computer Interfaces," 2006.

[11] L. A. Farwell and E. Donchin, "Talking off the top of your head: toward a mental prosthesis utilizing event-related brain potentials," in *Electroencephalography and clinical Neurophysiology*, Ireland, Elsevier Scientific Publishers, 1988, pp. 510-523.

[12] T. D'Albis, *A Predictive Speller for a Brain-Computer Interface based on Motor Imagery,* Milan: Artificial Intelligence and Robotics Laboratory of Politecnico de Milano, 2008.

[13] F. L. Nicolas-Alonso and J. Gomez-Gil, "Brain Computer Interfaces, a Review," *Sensors,* pp. 1211-1279, 2012.

[14] S. Sanei and J. A. Chambers, EEG Signal Processing, West Sussex, Chischester/Southern Gate: John Wiley & Sons Ltd, The Atrium,, 2007.

[15] E. Niedermeyer and F. L. Da Silva, Electroencephalography, Fifth ed., Philadelhia, Pennsylvannia: Lippincott Williams and Wilkins, 2005.

[16] E. Basar, EEG-Brain Dynamics, Amsterdam: Elsevier/North-Holland Biomedical Press, 1980.

[17] Natural Health School, "A Home Study Program in Herbalism, Nutrition and Natural Health," 16 07 2012. [Online]. Available: www.naturalhealthschool.com.

[18] H. H. Dr.Mueller, "Practice in Clinical and Health Psychology," 2012. [Online]. Available: http://www.drmueller-healthpsychology.com.

[19] M. Teplan, "Fundamentals of EEG Measurement," *Measurement Sicience Review,* vol. 2, 2002.

[20] BCI2000, "BCI 2000," July 2012. [Online]. Available: http://www.bci2000.org/.

[21] J. Malmivuo, "Bioelectromagentism," WebStat, 12 Febraury 2010. [Online]. Available: http://www.bem.fi/. [Accessed 20 July 2012].

[22] C. Brunner, "BCI Software Platforms," in *BCI Software Platforms*, Graz, Austria, 2005.

[23] Y. Rennard, F. Lotte, V. Delannoy, G. Gibert, E. Maby and M. Congendo, "OpenViBE: An Open Source Software Platform to Design, Use and Test Brain-Computer Interfaces in Real and Virtual Environments," *Presence Teleoperators & Virtual Environments,* 2010.

[24] W. v. Drongelen, Signal Processing for Neuroscientists, Amsterdam: Elsevier, 2008.

[25] P. Husar, Biosignalverarbeitung, Berling;Heidelberg: Springer-Verlag, 2010.

[26] S. M. Dunn, A. Constantinides and P. V. Moghe, Numerical Methods in Biomedical Engineering, London: Elsevier Academic Press, 2006.

[27] M. Werner, Digitale Signalverarbeitung mit MATLAB, Fifth ed., Wiesbaden: Vieweg + Teubner | Springer Fachmedien, 2012.

[28] B. Rivet, A. Souloumiac, V. Attina and G. Gibert, "xDAWN Algorthm to Enhance Evoked Potentials: Application to Brain Computer Interfaces," GIPSA-lab, Grenoble Institute of Technology, Grenoble, 2009.

[29] M. Vinther, "Improving Evoked Potential Extraction," Logicnet, Orsted, 2002.

[30] E. Donchin, M. K. Spencer and R. Wijesinghe, "The Mental Prosthesis: Assessing the speed of a P300-Based Brain-Computer Interface," *IEEE*

*Transactions on Rehabilitation Engineering,* vol. 8, no. 2, pp. 174-179, June 2000.

[31] H. Cecotti and A. Gräser, "Time Delay Neuro Network with Fourier Transform for Multiple Channel Detection of Steady State Visual Evoked Potentials for Brain Computer Interfaces," Lausanne, 2008.

[32] F. Bießmann, "New Methods for the P300 Visual Speller," Dept. Empirical Inferences, MPI for Biological Cybernetics, Tübingen, 2006.

## List of Figures

## List of Tables

# APPENDIX

## A.1 Acquisition Hardware

A 

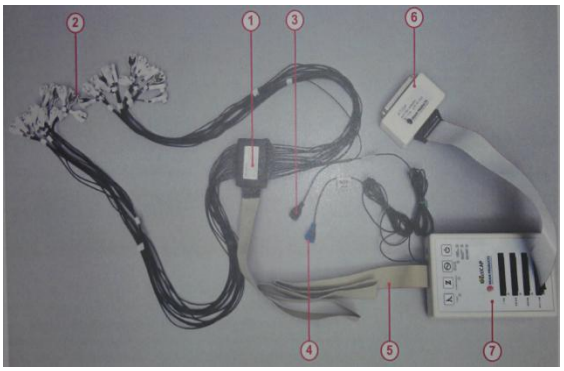

B

C 



D

The pictures show the main Hardware used for signal acquisition in the experiments.

A and B show the actiCAP electrode system consisting of the following:

- In A: The cap, conducting gel and syringe in picture A
- In B: (1) splitter box (2) 32 active electrodes (3 &4) ground and reference electrodes (5) actiCAP connector (6) amplifier adapter (7) actiCAP control box[8]

In C: The 32-channel TMSi analog to digital converter

In D: Desktop Computer[9].

[8] Picture taken from the actiCAP user Manual by Brain Products
[9] Picture taken from www.blogspot.de

## A.2 Setting up the experiment and dealing with Impedance

**E**   **F**

**Picture E:** a mounted actiCAP with the electrodes connected to the powered control box. The red light of the LED indicates high impedance of skin-electrode medium (see 3.2.1)

**Picture F:** applying conducting gel through opening in the electrode head to reduce impedance. When the LED light changes from red through yellow to green, the operating impedance of the electrode has been attained[10].

[10] Picture taken from actiCAP user manual by Brain Products.